2023

Confounding effects of snow cover on remotely sensed vegetation indices of evergreen and deciduous trees: An experimental study

R. Wang

K. R. Springer

John A. Gamon
University of Nebraska-Lincoln, jgamon@unl.edu

RESEARCH ARTICLE

Global Change Biology WILEY

Confounding effects of snow cover on remotely sensed vegetation indices of evergreen and deciduous trees: An experimental study

Ran Wang[1] | Kyle R. Springer[2] | John A. Gamon[1]

[1]School of Natural Resources, University of Nebraska-Lincoln, Lincoln, Nebraska, USA

[2]Department of Biological and Environmental Sciences, Concordia University of Edmonton, Edmonton, Alberta, Canada

Correspondence
Ran Wang and John A. Gamon, School of Natural Resources, University of Nebraska-Lincoln, Lincoln, NE, USA.
Email: ranwangrs@gmail.com and jgamon@gmail.com

Abstract

Located at northern latitudes and subject to large seasonal temperature fluctuations, boreal forests are sensitive to the changing climate, with evidence for both increasing and decreasing productivity, depending upon conditions. Optical remote sensing of vegetation indices based on spectral reflectance offers a means of monitoring vegetation photosynthetic activity and provides a powerful tool for observing how boreal forests respond to changing environmental conditions. Reflectance-based remotely sensed optical signals at northern latitude or high-altitude regions are readily confounded by snow coverage, hampering applications of satellite-based vegetation indices in tracking vegetation productivity at large scales. Unraveling the effects of snow can be challenging from satellite data, particularly when validation data are lacking. In this study, we established an experimental system in Alberta, Canada including six boreal tree species, both evergreen and deciduous, to evaluate the confounding effects of snow on three vegetation indices: the normalized difference vegetation index (NDVI), the photochemical reflectance index (PRI), and the chlorophyll/carotenoid index (CCI), all used in tracking vegetation productivity for boreal forests. Our results revealed substantial impacts of snow on canopy reflectance and vegetation indices, expressed as increased albedo, decreased NDVI values and increased PRI and CCI values. These effects varied among species and functional groups (evergreen and deciduous) and different vegetation indices were affected differently, indicating contradictory, confounding effects of snow on these indices. In addition to snow effects, we evaluated the contribution of deciduous trees to vegetation indices in mixed stands of evergreen and deciduous species, which contribute to the observed relationship between greenness-based indices and ecosystem productivity of many evergreen-dominated forests that contain a deciduous component. Our results demonstrate confounding and interacting effects of snow and vegetation type on vegetation indices and illustrate the importance of explicitly considering snow effects in

---

any global-scale photosynthesis monitoring efforts using remotely sensed vegetation indices.

1 | INTRODUCTION

The boreal zone covers about 1.89 billion ha in the northern hemisphere and is defined as the high northern latitude broad vegetation zone that is covered principally with forests, wetlands, lakes, and rivers (Brandt et al., 2013). Boreal forest function and health, including photosynthesis and respiration, are closely linked to temperature and precipitation patterns (Bonan, 2008). Altered growing season temperature and moisture availability with changing climate will lead to further effects on plant productivity (Bunn et al., 2007). Warmer temperatures are likely to cause an earlier spring onset and a delayed fall decline in photosynthesis. Thus, forests may yield greater carbon uptake and productivity as a result of a longer period with green foliage and an extended period of favorable conditions (Estiarte & Peñuelas, 2015). While boreal species can show positive photosynthetic and growth responses to warming (Way et al., 2015; Way & Oren, 2010), warmer temperatures also lead to higher respiration (Dunn et al., 2007) and influence the frequency and severity of disturbances such as drought, fire, or insect infestation, which directly impact vegetation succession and reduce ecosystem productivity (Dial et al., 2022; Moreau et al., 2020; Walker & Johnstone, 2014; White et al., 2017). Changing climate also alters snow cover (IPCC, 2007), potentially affecting the ability of remote sensing to assess changing vegetation productivity (Myers-Smith et al., 2020). Together, these effects lead to considerable uncertainty in the prediction of ecosystem productivity in a changing world.

Remote sensing provides a means of monitoring plant physiological and phenological processes at multiple spatial and temporal scales. Vegetation indices derived from optical remote sensing have been widely used to monitor photosynthetic phenology of different terrestrial ecosystems (DeFries & Townshend, 1994; Running et al., 2004; Schimel et al., 2015; Schimel & Schneider, 2019). For example, utilizing reflectance in the red and near-infrared bands, the normalized difference vegetation index (NDVI; Tucker, 1979) provides an estimate of vegetation greenness. NDVI can be used as an indicator for seasonal phenology of green biomass, leaf display, and photosynthesis for annual and deciduous species, but the NDVI–photosynthesis relationships are less clear for evergreen species (Gamon et al., 1995). Studies have used NDVI or similar indices as direct productivity indicators (Myneni et al., 1997) or as an input parameter to drive productivity estimation models (Goetz et al., 2005; Running et al., 2004). Such greenness indices, including NDVI, the enhanced vegetation index (Huete et al., 2002) and the newly developed near-infrared reflectance of vegetation (NIRv; Badgley

et al., 2017, 2019), largely fail to detect changes in photosynthetic activity in evergreen species that undergo seasonal downregulation and upregulation without apparent changes in canopy structure (Gamon et al., 1995, 2015, 2016; Springer et al., 2017; Wang et al., 2023; Zeng et al., 2022). This limitation has led to the development of additional indices that are more directly related to the actual photosynthetic regulatory processes invisible to NDVI and similar greenness indices.

The photochemical reflectance index (PRI) is capable of detecting these subtle changes in foliage relating to the regulation of photosynthetic activity (Gamon et al., 1992, 1997). On shorter (diurnal) time scales, PRI changes are driven by changes in xanthophyll cycle pigments, including violaxanthin, antheraxanthin, and zeaxanthin. Xanthophyll cycle activity leads to dissipation of excess light energy as heat, and the quenching of fluorescence via non-photochemical quenching, thereby protecting the photosynthetic apparatus (Demmig-Adams & Adams, 1996; Jahns & Holzwarth, 2012; Niyogi et al., 1997). For evergreens, zeaxanthin and other carotenoid levels remain high during cold period, maximizing dissipation of light energy to protect leaves during winter (Adams III et al., 2002; Öquist & Huner, 2003). In this case, PRI variation over long time periods is influenced by the seasonal change in leaf pigment pool sizes (Gamon & Berry, 2012; Garbulsky et al., 2011; Hmimina et al., 2014; Wong & Gamon, 2015a, 2015b), which are closely tied to seasonal gross primary productivity (GPP) patterns (Wong et al., 2020). Consequently, PRI can indicate both short-term (e.g., diurnal) downregulation due to xanthophyll cycle pigment activity, and longer-term (e.g., seasonal) adjustments in photosynthetic activity due to adjustments in photosynthetic and photoprotective pigment pools. The sensitivity to subtle changes in pigments makes PRI a powerful tool to monitor photosynthetic phenology of evergreen species (Wong et al., 2019, 2020; Wong & Gamon, 2015b). However, the application of PRI in tracking boreal forest phenology at global scales is currently limited by the lack of suitable bands in most current satellite sensors.

The chlorophyll/carotenoid index (CCI), which utilizes MODIS bands 1 and 11, has been proposed as an alternative indicator of photosynthetic activity, particularly for evergreen species (Gamon et al., 2016). Like the PRI, CCI is sensitive to changes in pigment pool sizes and can accurately track seasonally changing chlorophyll/carotenoid levels and photosynthetic activity at both the leaf and stand level over seasonal courses (Gamon et al., 2016; Pierrat, Magney, et al., 2022; Wong et al., 2019, 2020, 2022; Yang et al., 2020, 2022). Consequently, CCI can be a useful indicator of altered photosynthetic activity tied to seasonally changing chlorophyll and carotenoid

pigment pools, particularly for evergreens where greenness-based indices (e.g., NDVI) work poorly.

Together, the combination of vegetation indices, such as NDVI, PRI, and CCI, can provide complementary information about monitoring ecosystem productivity phenology of evergreen and deciduous forests (Gamon, 2015). For deciduous species, NDVI is closely related to the fraction of absorbed photosynthetically active radiation and allows monitoring of changes in canopy greenness, such as leaf development in the spring and senescence and abscission in the fall (Balzarolo et al., 2016). In contrast, evergreen species maintains their needles through the year and show little variation in canopy greenness (Hmimina et al., 2013; Wu et al., 2014). In this case, the carotenoid sensitive indices (PRI and CCI) can be directly linked to evergreen productivity and used to estimate photosynthetic light use efficiency (Springer et al., 2017; Wong et al., 2020, 2022). The integration of vegetation indices enables us to detect contrasting, complementary physiological, and structural controls of productivity for deciduous and evergreen species.

Despite the widespread use of satellite remote sensing techniques for studies of changing global productivity, few of these studies explicitly consider snow effects on estimates of changing productivity. Changing patterns of winter snow cover in the northern latitude and high elevation regions can influence ecosystem productivity estimation using satellite optical measurements due to the high visible reflectance of snow (Gamon et al., 2013; Jin et al., 2017; Jin & Eklundh, 2014; Springer et al., 2017), which alters different spectral regions to different degrees (Negi et al., 2009; Saha et al., 2019; Singh et al., 2010). These effects can readily alter the values of reflectance indices and confound interpretation of changing function in northern latitude ecosystems (Myers-Smith et al., 2020), yet this issue is rarely clearly addressed in most satellite-based studies that use reflectance-based vegetation indices. Similarly, the interaction of vegetation type with snow cover is not entirely clear, although considerable evidence exists to suggest that snow cover effects vary between different vegetation types (Bokhorst et al., 2016; Marsh et al., 2010). Given the complexities of varying vegetation type and snow cover, it is possible that varying snow cover can explain at least part of the widely reported failure for models to reliably depict the seasonal course of GPP (e.g., Keenan et al., 2012; Richardson et al., 2012; Rogers et al., 2022; Schaefer et al., 2012), particularly during transitional spring conditions.

The normalized difference snow index (NDSI) derived from the MODIS data utilizes the green and short-wave infrared bands and can be used to estimate snow coverage at continental and global scales (Riggs et al., 2016). However, the application of NDSI is limited by the malfunction of Aqua SWIR detectors (Gladkova et al., 2012) and its sensitivity to low solar irradiance caused by large solar zenith angle or at complex landscapes (Lv & Pomeroy, 2019; Wang et al., 2018). Despite the efforts in developing vegetation indices that may be less sensitive to snow cover (Camps-Valls et al., 2021; Jin et al., 2017), there are few explicit studies of snow effects on reflectance indices. These effects of snow cover have been primarily considered for some more common indices (e.g., NDVI; Gamon

et al., 2013; Myers-Smith et al., 2020), but less studied for others (e.g., PRI and CCI), even though there is emerging evidence for such effects (Pierrat, Magney, et al., 2022).

Several recent studies have reported clear confounding effects of snow on vegetation indices from both tower-based measurements (Pierrat et al., 2021; Pierrat, Magney, et al., 2022) and satellite observations (Cheng et al., 2022; Gamon et al., 2013; Myers-Smith et al., 2020; Wang et al., 2023). The snow effects on vegetation indices vary among vegetation types (Pierrat, Magney, et al., 2022) and among sites representing different biomes (Wang et al., 2023) due to varying species composition, canopy structure, and environmental conditions. However, the overall influence of snow on remote observations of vegetation photosynthesis has not always been clearly addressed and a systematic experimental investigation of how snow influences different vegetation indices across vegetation types has been lacking.

In this study, we designed an experiment using leaf-level gas exchange and reflectance, canopy reflectance, and digital images of potted trees at the University of Alberta, Canada to understand how snow cover influences canopy reflectance and vegetation indices of several evergreen and deciduous boreal forest tree species. We also tested the complementarity hypothesis (Gamon, 2015; Gamon et al., 2016), which argues that different vegetation indices (e.g., NDVI and PRI) having contrasting sensitivity to canopy structure and physiology. Thus, different vegetation indices provide complementary information about plant photosynthesis. In particular, we hypothesize that (1) snow has substantial effects on vegetation indices and confounds the estimations of photosynthetic properties based on optical properties (further illustrated in Figure 2 below) and (2) effects of snow on vegetation indices vary among vegetation indices and between deciduous and evergreen species. Because the combined effects of snow and vegetation type are difficult to assess from satellite measurements at large spatial scales, an initial clarification of these effects in an experimental setting is a necessary first step toward improved global assessment of primary productivity based on vegetation indices.

2 | MATERIALS AND METHODS

2.1 | Experimental setup

We used six tree species that are commonly found in North American boreal forests, including three evergreen species (*Picea mariana*, *Picea glauca*, and *Pinus banksiana*) and three deciduous species (*Populus tremuloides*, *Populus balsamifera*, and *Larix laricina*). We grew six monocultures and three mixed stands—M-1 (*L. laricina*, *P. mariana*), M-2 (*P. tremuloides*, *P. banksiana*), and M-3 (*P. balsamifera*, *P. glauca*)—on the rooftop of the Biological Sciences Building at the University of Alberta, Canada (Latitude: 53.529°, Longitude: −113.526°; Figure 1). Trees were potted in 2.83 L deep pots in spring 2015 and repotted into 6.23 L pots in April 2016 (during a period of leaf flush) for adequate moisture and nutrient availability and to
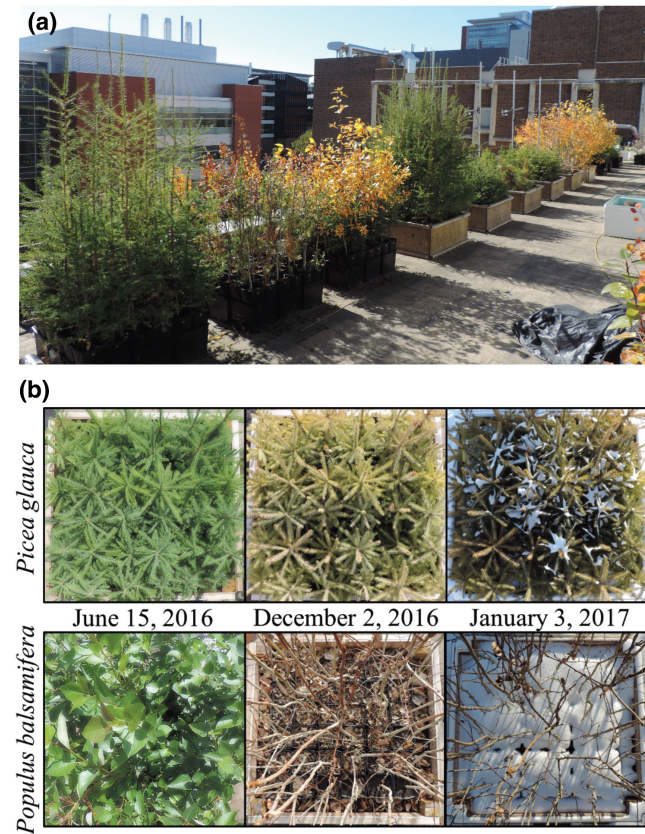
FIGURE 1 Experimental design. (a) Synthetic plots of boreal tree species established on the rooftop of the Biological Sciences Building, University of Alberta. Plots (from left to right) consist of three mixed stands M-1 (*Larix laricina*, *Picea mariana*), M-2 (*Populus tremuloides*, *Pinus banksiana*), and M-3 (*Populus balsamifera*, *Picea glauca*) and six monocultures including *L. laricina*, *P. mariana*, *P. banksiana*, *P. glauca*, *P. tremuloides*, and *P. balsamifera*. Photo was taken on September 28, 2017. (b) Representative evergreen (*P. glauca*) and deciduous (*P. balsamifera*) canopies of synthetic rooftop plots in summer (June 15, 2016), winter (December 2, 2016), and with snow cover in the winter (January 3, 2017).

avoid potential root restriction. During growing seasons, trees were watered daily and fertilized periodically to avoid water and nutrient deficits (Springer et al., 2017). An automated weather station was set up on the same rooftop where the trees were planted. Air temperature (S-THB-M002; Onset) and photosynthetic photon flux density (S-LIA-M003; Onset) were collected every minute and aggregated to 15-min averages.

2.2 | Gas exchange

Photosynthetic rate, expressed as net CO_2 assimilation, was measured using a portable gas exchange system (LI-6400; LI-COR). Leaves, or bundles of leaves in the case of conifers, were placed inside a $6\,cm^2$ leaf gas exchange chamber (6400-02B; LI-COR). The chamber monitored CO_2 assimilation rates under $1500\,\mu mol$ photons $m^{-2}\,s^{-1}$ to determine light-saturated photosynthetic rate ($\mu mol\ CO_2\ m^{-2}\,s^{-1}$). Light saturation

was confirmed through light-response curves that were performed on each species in July 2016 (Springer, 2018). The reference CO_2 was set to $400\,\mu mol\,mol^{-1}$ to match atmospheric concentrations. The chamber air flow was set to $400\,\mu mol\,s^{-1}$, with temperature and humidity set to match ambient conditions. Following a 1–3 min acclimation period after the leaf clip was set on a plant, five consecutive measurements were taken from a single branch or leaf on each plant from a total of five plants of each species. The photosynthetic rate of each species at the plot level was determined by averaging the measurements ($N = 25$) from all individuals of a given species at a single sampling interval. Leaf area for broadleaf species (*P. tremuloides* and *P. balsamifera*) was determined by the $6\,cm^2$ leaf chamber area; for needle-leaved species, leaf area was determined from the size (length and width measured by a caliper) and number of needles present in the gas chamber during sampling. For each species, mature leaf tissues were sampled whenever possible; new tissues were sampled for *P. mariana* and *P. glauca* during the spring of 2016 when the elongation of new branches did not allow for sampling of mature sun-lit tissues. For evergreen species, gas exchange data were collected from December 2015 to February 2017 approximately every 2 weeks. For deciduous species, gas exchange data were sampled between April 2016 (noticeable leaf-out) and October 2016 (full leaf senescence) at the same frequency. Gas exchange measurements were only collected for plants in the six monoculture plots but not for the same species in the mixed stands due to the time required for multiple gas exchange measurements.

2.3 | Leaf reflectance

Leaf reflectance was taken using a single-channel spectrometer (Unispec; PP System) coupled with a needle leaf clip (UNI501; PP System) with an internal halogen light source. The needle leaf clip allowed a narrow field of view (0.6-mm-diameter), which enabled sampling of small, narrow needle leaves. We randomly sampled five leaves for each plant and five plants for each species, for a total of 25 samples per species. For each plant, leaf measurements were preceded with a dark and a white reference scan (Spectralon; Labsphere). Leaf reflectance was calculated by dividing each leaf measurement by a white reference scan after subtracting a dark spectrum from each measurement. The spectrometer has a nominal spectral range from 350 to 1100 nm with 2–3 nm sampling intervals and 10 nm full width at half maximum (FWHM). A linear interpolation was used to estimate reflectance at 1-nm intervals. Leaf reflectance was measured on the same dates when gas exchange data were collected. Leaf reflectance was only collected for plants in the six monoculture plots but not plants in the mixed stands. This leaf reflectance dataset (Wang et al., 2016a) is available at the EcoSIS Spectral Library (ecosis.org).

2.4 | Canopy reflectance

Canopy reflectance was taken using a dual-channel spectrometer (Unispec DC; PP System). A downward looking fiber (Field of View
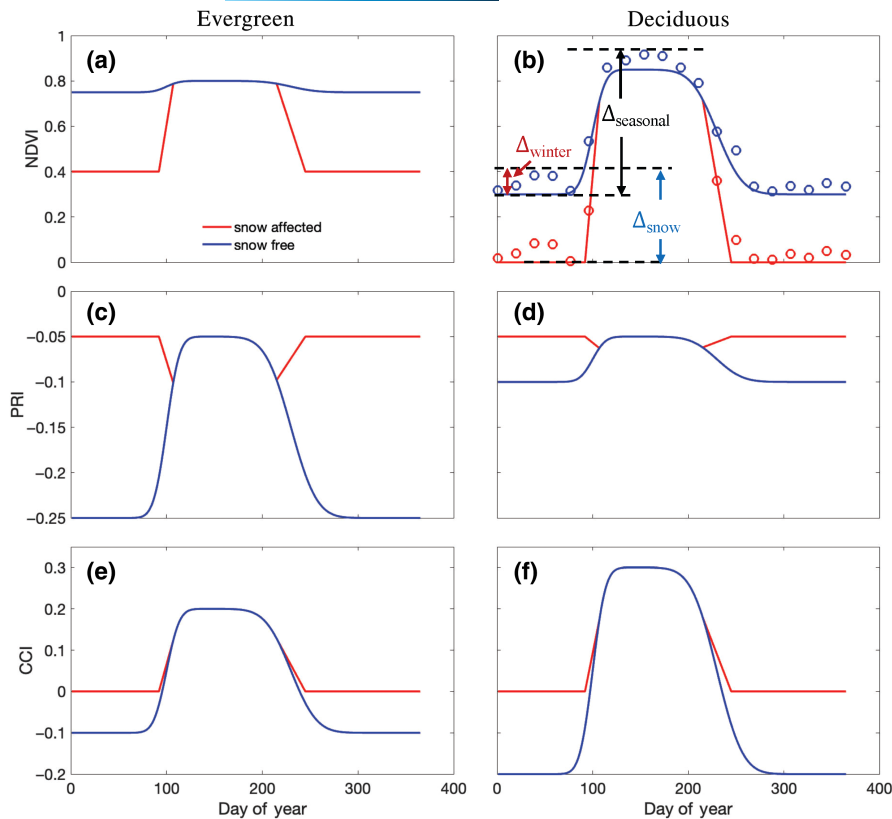
FIGURE 2 Conceptual figure indicating how snow influences the vegetation indices for evergreen (a, c, e) and deciduous (b, d, f) tree canopies. The blue line denotes the hypothetical seasonal vegetation index trend without snow, while the red line denotes the snow-affected vegetation index in the winter period. The calculations of seasonal ($\Delta_{seasonal}$), winter (Δ_{winter}), and snow (Δ_{snow}) deltas are illustrated in panel (b), which overlays hypothetical data points on the hypothetical trends.

approximately 20°) was used to measure the reflected radiance from the target and an upward looking fiber that connected to a cosine header (UNI435; PP Systems) was used to measure the incoming irradiance. The detector measured irradiance and radiance from 350 to 1100 nm with 10 nm spectral resolution (FWHM) and 2–3 nm sampling intervals. Canopy reflectance were collected for all the plots, including monocultures and mixed stands. Five measurements were taken for each of the nine treatment plots at different locations (center, NW, NE, SW, and SE; Springer, 2018) ca. 1 m above the top of the canopy and averaged as the reflectance of the plot. The reflectance data were cross-calibrated using measurements of a white reference panel (Spectralon; LabSphere) prior to sampling of each plot. This dual-channel design allowed us to compensate for any slight changes in sky conditions, during the reflectance sampling period (Gamon et al., 2006). Canopy reflectance was measured between December 2015 and February 2017 on an approximately 2-week basis and was taken under sunny days and within 1 h of solar noon on each sampling day. We typically measured the canopy reflectance within 3 days of the leaf-level measurements. This canopy reflectance dataset (Wang et al., 2016b) is available at the EcoSIS Spectral Library (ecosis.org).

We calculated three vegetation indices that are commonly used to monitor photosynthetic phenology of boreal forests, including NDVI, PRI, and CCI at both leaf and canopy levels using directly measured leaf and canopy reflectance, respectively, as:

$$NDVI = \frac{\rho_{800} - \rho_{630}}{\rho_{800} + \rho_{630}}. \tag{1}$$

$$PRI = \frac{\rho_{531} - \rho_{570}}{\rho_{531} + \rho_{570}}. \tag{2}$$

$$CCI = \frac{\rho_{531} - \rho_{630}}{\rho_{531} + \rho_{630}}. \tag{3}$$

2.5 | Quantifying snow effects on seasonal changes in VIs

We quantified the snow effects on vegetation indices by calculating the seasonal change in vegetation indices with and without snow present (Figure 2). During snow-covered periods, temperatures were typically below or near 0°C and there was no measurable photosynthesis (Springer et al., 2017; Wong & Gamon, 2015a). Thus, we used two snow-free dates in the winter (January 29, 2016 and November 7, 2016) as "zero" snow cover points that provided "base line" values for vegetation indices without snow contamination or detectable photosynthetic activity. We then calculated the *seasonal deltas* ($\Delta_{seasonal}$) of vegetation indices as difference between the maximum and minimum extremes for the snow-free data collected in 2016, which captured the seasonal biological effect on vegetation indices apart from any snow influence. The *snow deltas* (Δ_{snow}), captured the direct effects of snow on vegetation indices, were calculated between the maximum and minimum extremes for all the data collected in winter (November 2015–March 2016). We also calculated *winter deltas* (Δ_{winter}) between the maximum and minimum extremes for all the snow-free data collected in winter (November 2015–March 2016), which captured the winter variation in vegetation indices apart from any snow effects and was typically close to zero.

2.6 | Quantifying snow effects on VIs by calculating snow percentage cover using digital images

To independently quantify the snow percentage cover, we took photographs of each monoculture plot from a height of approximately 1.5 m above the canopy on the same dates that we sampled the canopy reflectance using a digital camera (Nikon Coolpix 520; Nikon Canada Inc). We trained a binary support vector machine (SVM) classifier using the *fitcsvm* function in MATLAB (2022) to identify snow pixels from each image, because supervised classification can yield more accurate snow cover estimations than methods based on applying thresholds on RGB bands (Fedorov et al., 2016). To train the binary SVM model, we selected four images that had different levels of snow coverage on both deciduous and evergreen species and visually identified snow and non-snow cover pixels. We cropped each image by using 30% of the shorter edge (height or width) at each side from the center of the image to only use the center portion of each image to estimate the snow percent cover to avoid distortions at the edges (Liu & Pattey, 2010). We tested the SVM classification accuracy using 10-fold cross-validation. The overall accuracy of snow identification using the binary SVM classification was 0.8. Most of the misclassified pixels occurred to pixels in shadows. We then applied the binary SVM model to the cropped images to calculate the snow percent cover of each image.

2.7 | Linking gas exchange to VIs at leaf and canopy levels

We used the leaf-level gas exchange data to establish the "biological baseline" for plants' seasonal photosynthetic rate variation. We then related vegetation indices at both leaf level and canopy level to the gas exchange data to investigate how different vegetation indices provide complementary information about plant photosynthetic activities of deciduous and evergreen species at different scales. The comparison between gas exchange data and vegetation indices at leaf and canopy levels also enabled us to evaluate how snow influenced the canopy-level vegetation indices for both evergreen and deciduous species. We compared leaf-level vegetation indices to canopy-level vegetation indices to test how the different vegetation indices can be scaled from leaf to canopy scale. To further examine the snow effects on phenology of the vegetation indices, we used asymmetric Gaussian functions (Jönsson & Eklundh, 2004) to fit the snow-corrected data to estimate the theoretical seasonal snow-free vegetation index variations.

3 | RESULTS

3.1 | Snow effects on canopy reflectance and vegetation indices

Clear seasonal changes occurred in spectral reflectance due to both biological effects and snow (Figure 3). For evergreen species, the pattern of winter canopy reflectance measured during the snow free period exhibited a clear difference from the summer reflectance, shown as lower reflectance values in the green wavelengths and higher reflectance values in the red wavelengths (Figure 3). Evergreen reflectance changes were also visible in the near-infrared (NIR), with higher NIR reflectance in the winter, particularly for *P. banksiana* (Figure 3b). As expected, deciduous species showed more striking seasonal contrasts in reflectance, with higher visible reflectance in the red and blue regions, and lower NIR reflectance in winter (Figure 3d–f). For *Populus* spp., winter reflectance consisted of energy scattered from branches and soil background. *L. laricina*, a deciduous conifer, had some dry yellow needles remained on the branches over the winter period, leading to higher NIR reflectance than *Populus* spp., but also higher reflectance in the visible (VIS) wavelengths (particularly in the red region) than the evergreen species (Figure 3). Snow strongly increased canopy reflectance across all spectral bands, and this increase varied with wavelength, decreasing the difference between VIS and NIR bands (Figure 3).

Along with these reflectance changes, canopy-level vegetation indices of different species varied across season and were clearly influenced by snow (Figure 4). Snow shifted the vegetation indices from measurements taken during winter dormancy, with sharp decreases in NDVI values and abrupt increases in PRI and CCI values during periods of snow (Figure 4). For evergreens, snow was the predominant influence on NDVI (Figure 4a). In deciduous species, snow led to a "two-step" shape in the winter–spring NDVI time series for the deciduous species, clearly showing the two causes (snow melt and green up) of changes in the spring NDVI values (Figure 4b). Compared to deciduous species, limited seasonal variations in NDVI occurred in evergreen species potentially due to biological effects (changing pigmentation or leaf area index). The slight drop in canopy-level vegetation indices in April 2016 was caused by repotting trees during a period of leaf flush (Figure 4).

Using "delta values" (defined in Figure 2), we explored the relative contribution of snow and biological effects on the reflectance indices (Figure 5). For all three vegetation indices, wintertime changes due to the variable presence of snow ("snow" delta values, $N=8$) were much greater than normal winter variability ("winter" delta values, $N=3$ but in different months) without snow (i.e., due to biological effects alone, which were minimal in winter). For evergreen species, snow caused a variation in NDVI that was four to six times larger than the typical seasonal variation ("seasonal" delta values) calculated when snow-affected period was excluded (Figure 5). In deciduous and mixed stands, the effect of snow on NDVI was smaller than the seasonal variation due to biological effects ("seasonal" delta values), but still yielded changes that were 40%–60% as large as the biological effects. For mixed stands, the snow effect on NDVI (expressed as "snow" delta values) was roughly equivalent to that of the biological effects ("seasonal" delta values; Figure 5).

The variation in PRI caused by snow was at a level that was comparable to the seasonal PRI variation for evergreens and mixed stands but was slightly smaller than biological PRI variation ("seasonal" deltas) for deciduous stands (Figure 5). In the case of CCI, snow effects were approximately half those of seasonal variation
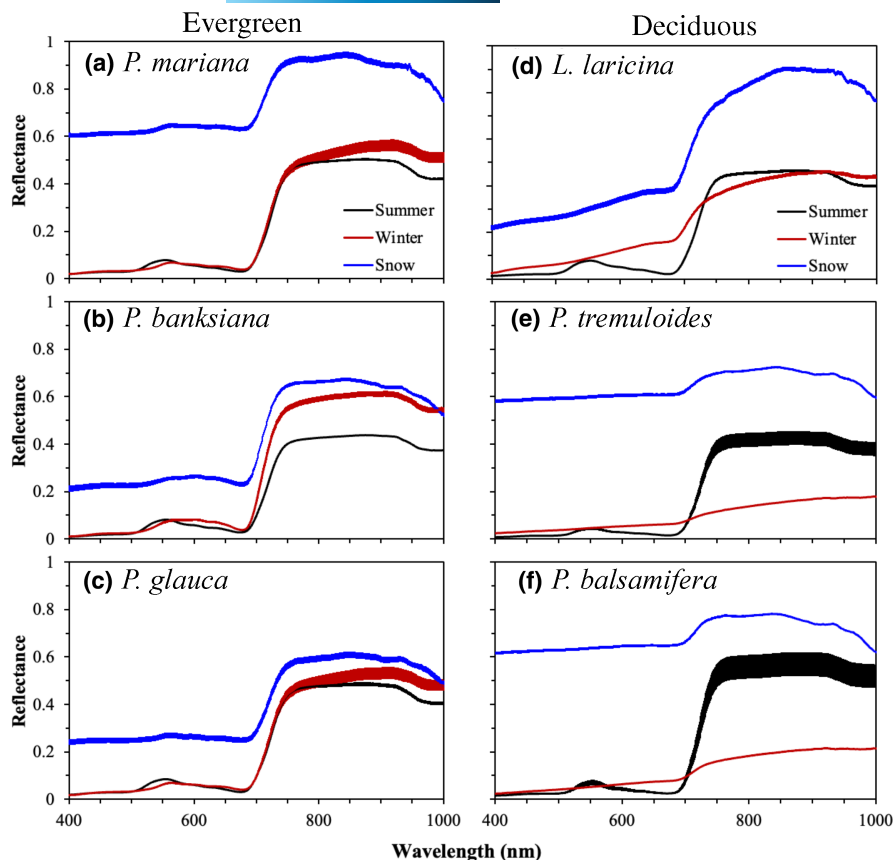
FIGURE 3 Canopy spectra of evergreen (a–c) and deciduous (d–f) monocultures in summer (black line) and winter (snow free period: red line and snow-affected period: blue line). Representative dates were chosen to depict reflectance spectra from summer (June 15, 2016), winter (December 2, 2016), and with snow cover on canopies (January 3, 2017). Width of the line denotes ±SE of the mean.

due to biological effects ("seasonal" deltas), indicating that while this index was least affected by snow, the effect was still substantial. Only minor changes were noticed in the vegetation indices during the winter snow-free period ("winter" deltas, Figure 5), indicating limited biological changes due to physiological or canopy structural changes during the winter.

3.2 | Correcting for snow effects on canopy level vegetation indices

The snow percent cover data obtained from the digital images during winter period also allowed us to quantify how snow-affected vegetation indices differently among species and functional types apart from any seasonal effects due to changing photosynthetic activity (Figure 6). Two snow free dates in the winter (January 29, 2016 and November 07, 2016) were used as "zero" snow cover point that provided baseline values for vegetation indices without snow contamination. Overall, stronger relationship (larger R^2) between vegetation indices and snow cover was found in deciduous than evergreen, while sharper changes (steeper slopes, $p < .001$) in NDVI and PRI with increasing snow percent cover were found in evergreen species than deciduous species (Figure 6a,b). The different slopes for PRI and NDVI indicated strong interactive effects of snow and vegetation type on these indices. For CCI, a larger intercept ($p < .001$) occurred for deciduous species than evergreen species, but the slopes were not significantly different between the two vegetation types ($p = .991$).

3.3 | Linking gas exchange to VIs at leaf and canopy levels

For evergreen species, photosynthetic activation began in March, with photosynthetic rates increasing to summer maxima by mid-June (Figure 7a). Following the growing season maxima, photosynthetic rates gradually decreased, reaching near zero again by November. During the spring transition, a large drop in photosynthetic rate was observed for the spruce species (*P. mariana* and *P. glauca*) that coincided with the sampling of newly emerged branches following budburst; this drop was not seen in *P. banksiana* as only mature needles of this species were sampled through the transition.

For deciduous species, rapid photosynthetic changes occurred in both spring and fall, with winter periods lacking foliage for sampling (Figure 7b). Spring transition of deciduous species started in April. *L. laricina* developed needles at the beginning of April and the *Populus* spp. unfolded their leaves within a relatively short period of time (between April 8 and April 18). In deciduous species, we missed sampling photosynthesis during the early spring transition following bud burst and early leaf development due to the relatively coarse sampling intervals and the difficulty of accurate measurements on small, emerging leaves (Figure 7b,d,f,h). Fall senescence of broadleaf species started at the end of August, indicated as a decrease in photosynthetic rate and leaf yellowing due to loss of chlorophyll (Figure 7b). At the end of September, few green deciduous leaves remained, which can also be confirmed by near-zero photosynthetic rates at this time (Figure 7b). Broadleaf species exhibited higher peak
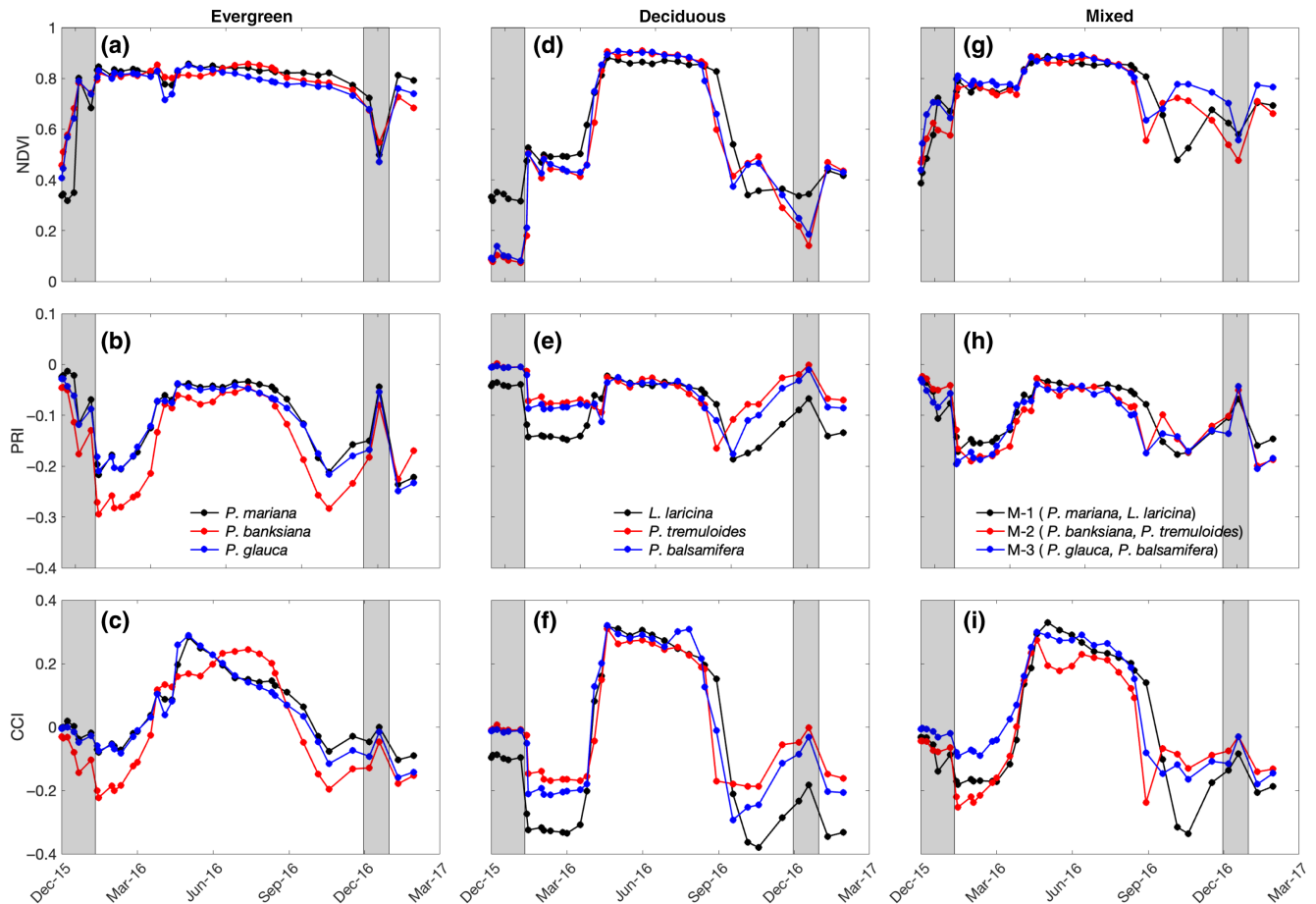
FIGURE 4 Seasonal patterns of canopy-level vegetation indices. Evergreen species (a–c) included *Picea mariana* (black), *Pinus banksiana* (red), and *Picea glauca* (blue). Deciduous species (d–f) included *Larix laricina* (black), *Populus tremuloides* (red), and *Populus balsamifera* (blue). Mixed stands (g–i) include M-1 (*P. mariana, L. laricina*), M-2 (*P. banksiana, P. tremuloides*), and M-3 (*P. glauca, P. balsamifera*). Gray-shaded areas denote snow-affected periods.

photosynthetic rates in the summer growing season and faster decreases in photosynthetic rate during the fall transition than *L. laricina*, a deciduous conifer.

The ability to use vegetation indices to track the seasonal photosynthetic rate varied among species and functional types (Figure 7). For evergreen species, clear seasonal patterns matching the trajectory of photosynthetic rates were exhibited by leaf-level PRI and CCI (Figure 7e,g). A slight seasonal variation of NDVI occurred in *P. banksiana* (pine) but not in the two *Picea* (spruce) species. During the wintertime, limited changes occurred in all three vegetation indices of the evergreens (Figure 7c,e,g). For deciduous species, clear seasonal patterns were found for all three vegetation indices tested, expressed as high values in the summer growing season and abrupt drops during the fall senescence (Figure 7d,f,h). *L. laricina*, a deciduous conifer, exhibited a more gradual change in vegetation indices during senescence than the broadleaf deciduous species.

For evergreen species, stronger relationships emerged between photosynthetic rate and PRI and CCI than between photosynthetic rate and NDVI (Figure 8; Table 1). The low photosynthetic rate obtained for the new needles of the two *Picea*

species in late April to early May affected the overall relationship between photosynthetic rate and vegetation indices, leading to outliers (Figure 8). Removing measurements of the *Picea* species for four outliers on April 20 and May 4 enhanced the relationship between photosynthetic rate and PRI and CCI (Figure 8; Table 1). Relationship between photosynthetic rate and NDVI changed slightly (Figure 8; Table 1).

For deciduous species, and especially for the two *Populus* species, limited variation in vegetation indices occurred during the summer growing season, but all vegetation indices yielded significant correlations with photosynthetic rate (Figure 7). For deciduous species, NDVI exhibited the closest relationship (largest R^2) with photosynthetic rate among the three vegetation indices tested (Table 1). This was the reverse of the pattern in the evergreens, where NDVI had markedly less variation with changing photosynthetic rates than PRI and CCI (Figure 8), illustrating the complementary nature of these indices in assessing photosynthetic activity for different vegetation types (Gamon, 2015; Gamon et al., 2016; Garbulsky et al., 2011).

Snow correction affected the relationship between photosynthetic rate and canopy vegetation indices and this snow effect varied among indices (Figure 9). Snow correction improved the relationship between
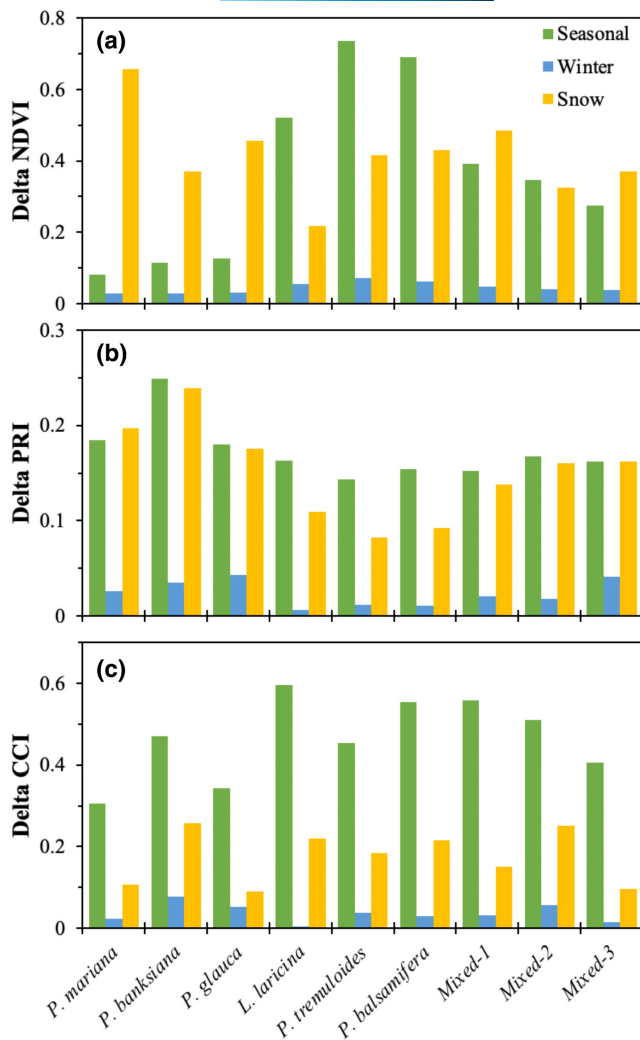
FIGURE 5 Delta vegetation index values, including NDVI (a), PRI (b), and CCI (c), for evergreen (left), deciduous (center), and mixed stands (right) on different temporal scales. Seasonal deltas (green) were taken from the maximum and minimum extremes from 2016, and represent the changes in index values due to biological effects during the growing season. Winter deltas (blue) were taken from the maximum and minimum extremes from November 2015 to March 2016 and represent the change in index values due to biological effects in the winter. Seasonal and winter deltas excluded data collected with snow present on canopies. Snow deltas (yellow) represent the changes in index values due to snow alone, and were taken from the maximum and minimum extremes from November 2015 to March 2016, and compare index values before and after snowfall. Calculation of these delta values are further explained in Figure 2.

FIGURE 6 Vegetation index (NDVI: a, PRI: b, and CCI: c) variation with snow percent coverage by canopy type (deciduous, evergreen, or mixed, represented as different colors). Snow percent coverage was estimated using digital images taken on the same days when canopy reflectance was sampled. The mixed plot data (blue points) are illustrated but not included in regressions. p-value $< .001$ for all the regressions. To isolate snow effects from biological effects, only winter data were used in this figure, assuming little change in physiology or structure during winter.

photosynthetic rate and PRI (expressed as higher R^2), while weakening the relationship between photosynthetic rate and NDVI, both of which represented artifacts of snow rather than actual biological effects. Snow cover had relatively little effect on the CCI–photosynthesis relationship (Figure 9; Table 1). We note that because most gas exchange measurements were limited to the growing season (Figure 7), a period with minimal snow cover, the effects of snow on these relationships were minimized in this figure. Because no leaf-level measurements
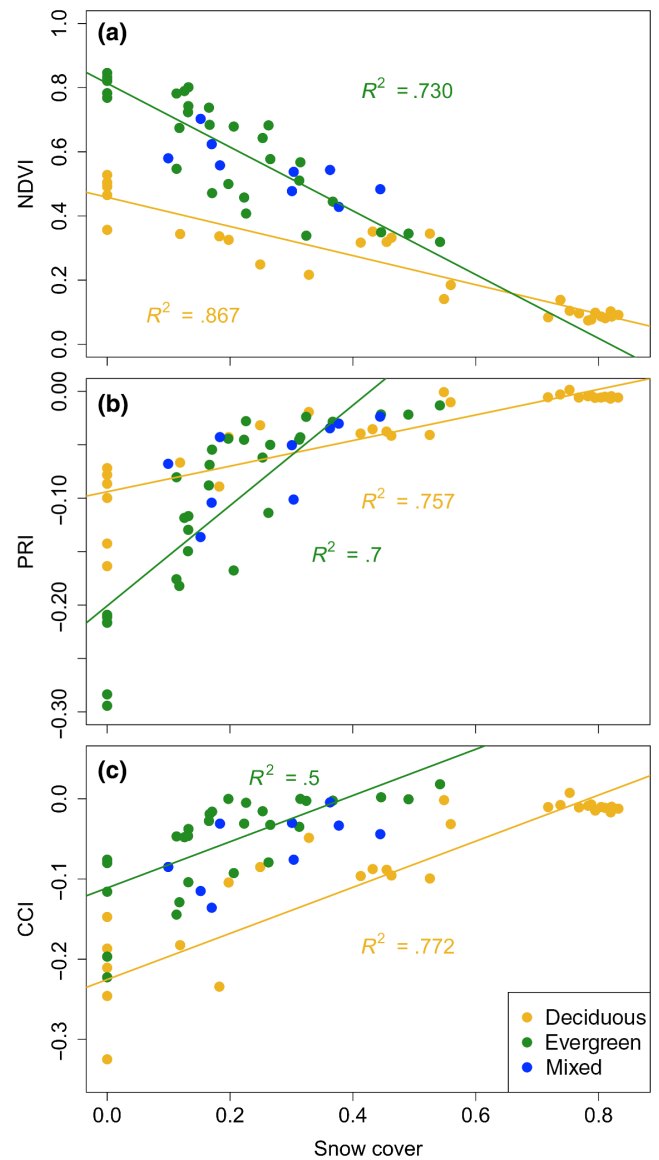
were collected for deciduous species during the snow-affected period (before bud burst and early leaf development), we evaluated the snow correction on canopy-level vegetation indices only for evergreen species in the following analysis.

Similar to the relationships between photosynthetic rate and vegetation indices at leaf level (Figure 8), the low photosynthetic rate of the two spruce species in late April and early May (Figure 7) also weakened the relationships between photosynthetic rate and vegetation indices at canopy scale (Figure 9). Removing measurements of two spruce species on April 20 and May 4 (during leaf flush)

FIGURE 7 Seasonal patterns of photosynthetic rate and leaf-level vegetation indices for evergreen (a, c, e, and g) and deciduous (b, d, f, and h) species. The period of new-leaf expansion (E) is labeled in panel (a).
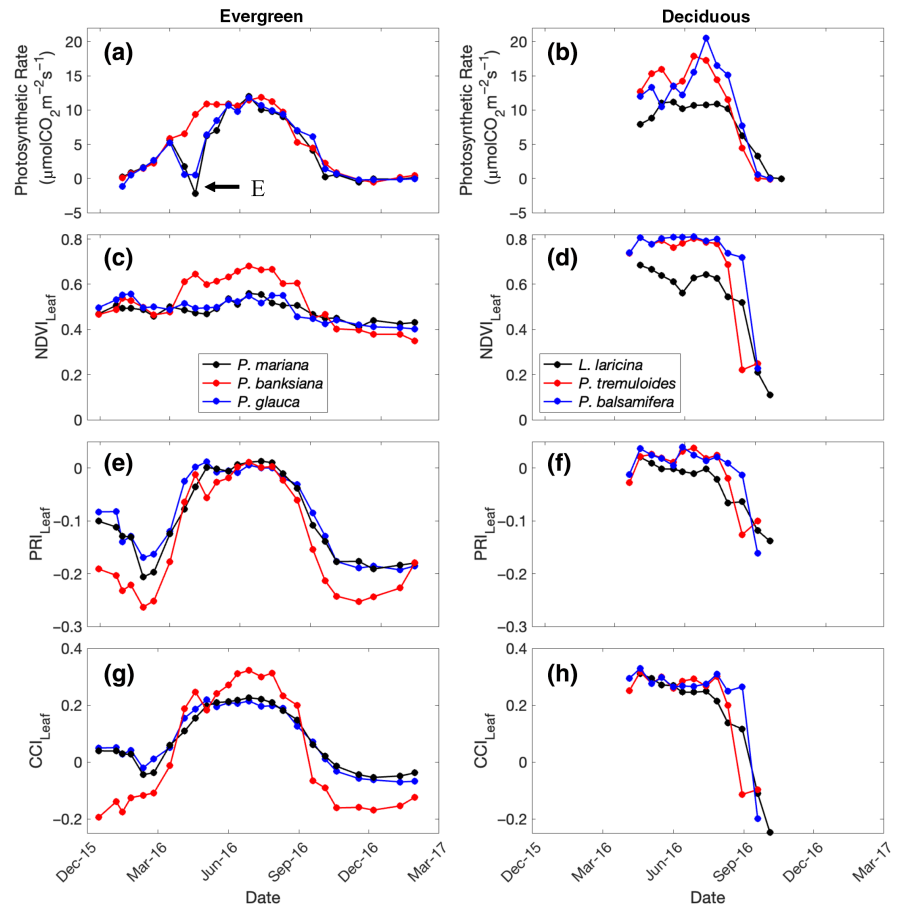
enhanced the relationship between photosynthetic rate and canopy PRI and CCI (Figure 9; Table 1).

To evaluate snow effects on scaling, we further compared the leaf-level vegetation indices to canopy-level vegetation indices directly (Figure 10). In all cases, snow correction improved the relationship between leaf-level and canopy-level vegetation indices (increased R^2, Figure 10). The agreement between leaf and canopy measurements (and indicator of "scalability") was strongest for PRI and CCI and weakest for NDVI (Figure 10). Leaf-level NDVI exhibited a much larger range than canopy-level NDVI, causing the NDVI plot to deviate markedly from the 1:1 line (Figure 10).

3.4 | Snow confounded vegetation phenology estimation using vegetation indices

Snow clearly confounded the fitted vegetation phenology curves using asymmetric Gaussian functions based on canopy-level vegetation indices (red curves, Figure 11). Snow correction removed the extremely low NDVI values and high PRI and CCI values in the snow-affected period, leading to phenology curves that presumably more closely fitted the biological influences due to pigmentation and green leaf area index (blue curves, Figure 11). For deciduous species, snow correction removed the initial increase exhibited in spring NDVI values caused by snow melt but not the increase due to biological effects, because snow melt happened prior to

bud burst, in a period when there were no leaves for the deciduous species (Figure 11). The large PRI and CCI values caused by snow influenced the performance of curve fitting algorithm by altering the minimum levels in the winter, leading to much smaller yearly variation in apparent phenology than would be the case in the absence of snow (Figure 11). Clearly, consideration of snow melt can have a large effect on the assessment of photosynthetic phenology using these vegetation indices.

We further summarized the snow effects on canopy-level vegetation index values, seasonal changes, and relationships between photosynthetic rate and vegetation indices in Table 2, which notes the contradictory responses of NDVI and the other indices (PRI and CCI) to snow.

4 | DISCUSSION

This experimental study demonstrated the impacts of winter snow cover on canopy reflectance and vegetation indices of deciduous and evergreen trees commonly found in North American boreal forests. Our results revealed clear snow cover effects on both spectral reflectance and vegetation indices (NDVI, PRI, and CCI) derived from optical sampling of canopies. These impacts varied with vegetation index, species, and functional types (evergreen and deciduous). This work complements other recent studies of snow effects on vegetation indices from satellite remote sensing at broader scales, revealing clear implications for estimates of global terrestrial vegetation productivity and phenology from
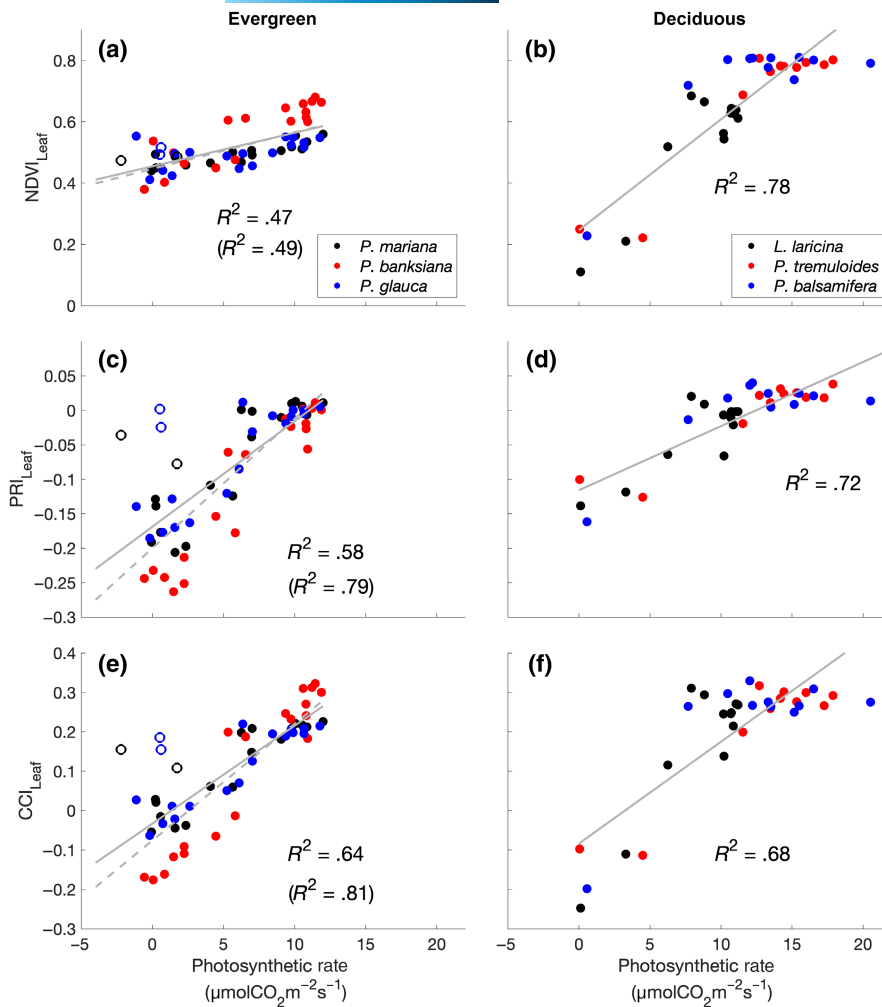
FIGURE 8 Relationships between photosynthetic rate and leaf-level vegetation indices for evergreen (a, c, e) and deciduous (b, d, f) species. Regressions (solid lines) were applied to combined evergreen and deciduous species, respectively. The outliers (*Picea* spp. on April 20 and May 4) are labeled as open symbols (panels a, c, e). Removing these outliers enhanced the relationship (dash line) between photosynthetic rate and PRI and CCI, as indicated in parentheses on the figures. Regression results are summarized as Table 1.

TABLE 1 Coefficient of determination (R^2) between photosynthetic rate and vegetation indices at leaf and canopy scales.

	Leaf level		Canopy level		
			Evergreen ($N = 53$)		
	Evergreen ($N = 53$)	Deciduous ($N = 34$)	Before snow correction	After snow correction	Deciduous ($N = 34$)
NDVI	0.47 (0.49)	0.78	0.22 (0.23)	0.17 (0.17)	0.71
PRI	0.58 (0.79)	0.72	0.51 (0.76)	0.55 (0.82)	0.58
CCI	0.64 (0.81)	0.68	0.55 (0.76)	0.55 (0.77)	0.65

Note: N denotes the sample size. p value < .001 for all regressions. At canopy level, regressions were only calculated for evergreen species to illustrate snow effects (before and after snow correction), because no photosynthesis measurements were collected for deciduous species during the snow-affected period. R^2 with *Picea* spp. outliers on April 20 and May 4 removed are shown in parentheses.

Abbreviations: CCI, chlorophyll/carotenoid index; NDVI, normalized difference vegetation index; PRI, photochemical reflectance index.

satellites using vegetation indices, all of which are confounded by snow. Our findings suggest substantial errors would result when estimating photosynthesis or GPP from reflectance-based indices, particularly during spring and fall when snow is more likely, unless snow effects are considered. Eliminating the contamination of snow on vegetation indices revealed the true "biological" baseline and enabled improved evaluation of seasonal patterns associated with biological changes.

4.1 | Snow effects on vegetation indices

The magnitude and patterns of changes in reflectance spectra in winter are largely influenced by vegetation canopy structure that impacts the retention and detection of snow in canopies (Pomeroy et al., 2002), and this varied with species and functional type. Among evergreens, different taxa (e.g., *Picea* spp. vs. *Pinus* spp.) vary in their ability to retain

FIGURE 9 Relationship between leaf-level photosynthetic rate and canopy-level vegetation indices for evergreen and deciduous species. The outliers (*Picea* spp. on April 20 and May 4) are labeled as open symbols and snow-affected data are labeled as stars. Solid and dash lines (panels a, c, e) indicate fitted lines before and after snow correction for evergreen species, respectively. R^2 for corrected relationships are in parentheses. R^2 for corrected relationships with outliers removed are in brackets. Regression results are summarized as Table 1.
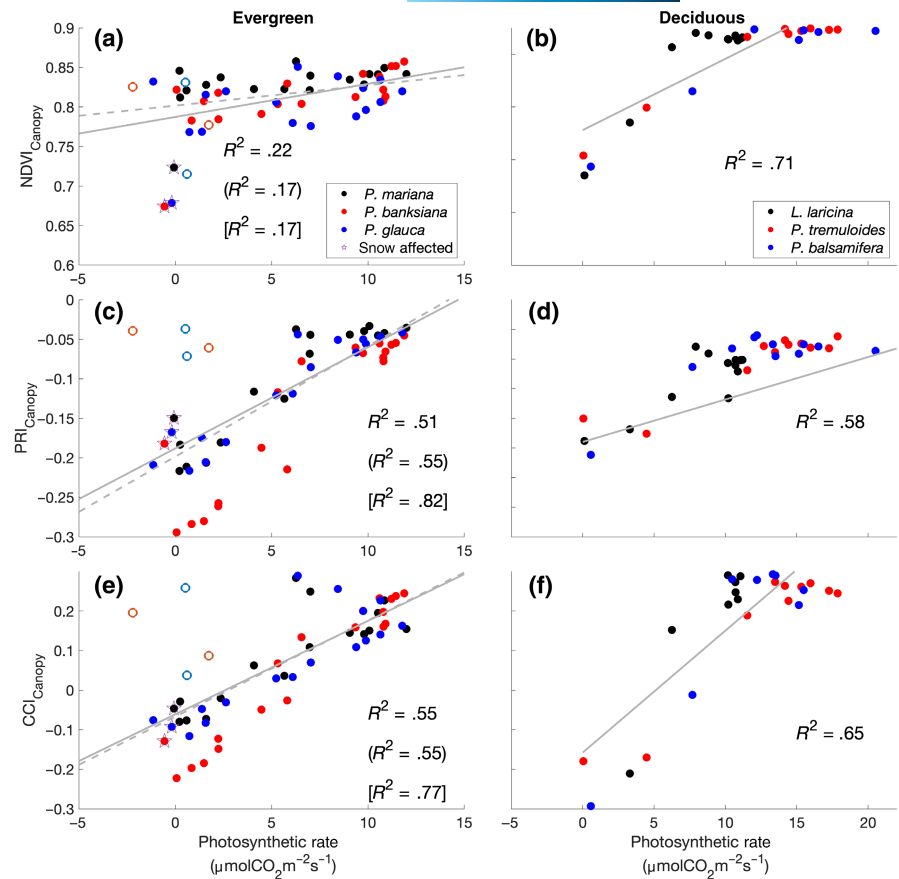
canopy snow, affecting vegetation indices to different degrees. The particular canopy branching pattern of *Picea* spp. retains snow much better than that of *Pinus* sp. confounding the remote monitoring of changes in photosynthetic activity for *Picea* spp. to a greater degree. On the other hand, the absence of winter foliage for deciduous species leads to the combination of snow-covered soil with bare stems and branches as influences on reflectance and vegetation indices (Figures 1 and 4). In natural landscape, deciduous branches may collapse and be buried beneath the snow cover, particularly for small trees or shrubs, influencing the overall optical signal of deciduous forests (Marsh et al., 2010; Ménard et al., 2014; Ray & Bret-Harte, 2022). Additionally, shrub branches can extend above the snowpack and alter albedo, surface temperature, and soil thermal regimes, which further accelerate snow melt (Myers-Smith & Hik, 2013; Pomeroy et al., 2006). These varying snow effects among evergreen and deciduous species can lead to variations in optical properties at broader scales (e.g., Cheng et al., 2022; Pierrat et al., 2021; Pierrat, Magney, et al., 2022), which would vary by species and vegetation type, in part due to varying snow retention.

Due largely to their different formulation using dissimilar spectral bands, contrasting vegetation indices were differentially affected by snow cover, indicating contradictory and confounding effects of snow on these indices (Figure 4; Table 2). These contradictory effects include exaggerated seasonal change (in the case of NDVI) and reduced seasonal change (in the case of PRI and CCI) and indicate artifacts in the sense they can easily lead to false conclusions regarding vegetation greenness, pigmentation, and photosynthetic activity. In accordance with previous studies (Eklundh et al., 2011; Gamon et al., 2013; Springer et al., 2017)

the fastest NDVI increases happened during the snow melt period in spring (Figure 4) when photosynthetic activity remained low. Additionally, without accounting for snow cover, NDVI can indicate a sharp decline in apparent "greenness" for deciduous species well after fall senescence and might incorrectly suggest a rapid loss or sudden emergence of green foliage in the winter for evergreens. Changes in NDVI due to differential snow cover in the early transition from winter to spring rival the magnitude of changes that coincide with bud burst and leaf flush for deciduous species and can far exceed that due to biological effects (due to canopy development or altered pigmentation) in evergreens (Figure 11). Together, these effects of snow on NDVI can lead to substantial errors in phenology estimation. Being inversely impacted by snow (relative to NDVI), PRI and CCI increases due to snow in wintertime to levels that are comparable to growing season maxima would suggest a sudden "turning on" of photosynthesis in the middle of winter for evergreens, and even deciduous species with no foliage. These results reveal clear and distinct artifacts of snow melt on vegetation indices apart from any direct effect of vegetation structure (e.g., leaf area index) or physiology (e.g., pigmentation and associated photosynthetic activity).

4.2 | Snow effects on estimation of vegetation photosynthetic activity and productivity

Remote sensing data can be used to quantify carbon fluxes through direct empirical relationships between vegetation indices and GPP, light use efficiency concepts, terrestrial biosphere models,
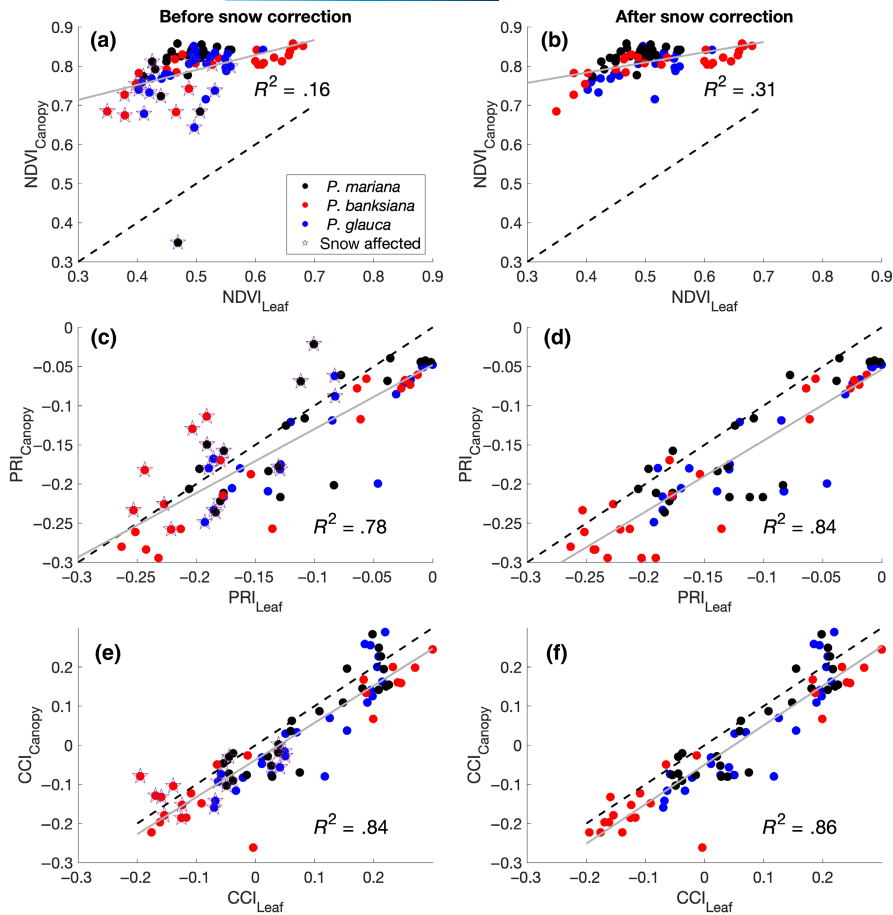
FIGURE 10 Snow correction enhanced the relationships between leaf-level and canopy-level vegetation indices (NDVI: a & b, PRI: c & d, CCI: e & f) for evergreen species. Canopy data with snow visible in the scene are labeled using stars. Solid line denotes the regression line and dash line indicates the 1:1 reference line. Regressions were fitted combining data from all three evergreen species.

or machine learning methods (reviewed in Ryu et al., 2019; Xiao et al., 2019). However, all reflectance-based vegetation indices commonly used for monitoring terrestrial ecosystem photosynthesis are sensitive to snow cover, especially for the high latitude and altitude areas, which endure long periods of winter snow (Eklundh et al., 2011). Compared to snow-affected data, NDVI exhibited limited seasonal variation for evergreen species, as expected based on previous studies quantifying NDVI phenology for evergreens in the absence of snow (e.g., Gamon et al., 1995). The small seasonal variation in NDVI for the evergreen species (Figure 5) is undoubtedly due to NDVI's sensitivity to green canopy structure (which has little seasonal change in evergreens). However, in northern latitude evergreen forests, greenness-based vegetation indices such as NDVI may exhibit strong relationships with GPP derived from eddy covariance measurements. Our results suggest that the strong relationship between GPP and greenness-based vegetation indices appears in part to be a "false signal" due to the confounding effects of snow and the coincidence of snow melt and snow fall with periods of photosynthetic activation and deactivation (Wang et al., 2023). The large errors in reflectance-based estimates of GPP during seasonal transitions (Keenan et al., 2012; Richardson et al., 2012; Schaefer et al., 2012), are likely partly attributable to such confounding snow effects.

The apparent seasonal response of greenness-based indices in evergreen forests can also be due to the significant contribution of

deciduous plants (including forest understory species) to surface reflectance. It has been reported that the forest understory, often including a large deciduous component, can account for about 61% total GPP in an Alaska black spruce forest (Ikawa et al., 2015). In such cases, the seasonal change in deciduous components can provide a considerable contribution to the overall remotely sensed optical signals (as illustrated by the mixed stands in this study), leading to strong relationships between NDVI-based indices and GPP in the boreal forests, despite snow artifacts. However, the confounding effects of snow on vegetation indices, which are clearly different for evergreen and deciduous species, are likely to complicate assessment of seasonal change from remote sensing in such mixed stands.

4.3 | Comparisons with natural landscapes

This experimental study allowed us to quantify snow effects on vegetation indices of deciduous and evergreen species and to separate snow artifacts from actual biological effects. While this study demonstrates the principles of snow effects on canopy reflectance and vegetation indices, the details would vary between this study and natural landscapes due in part to difference in species composition, canopy structure, and landscape effects (e.g., variation in topography and forest density). Our photosynthesis measurements were limited to periods of the growing season
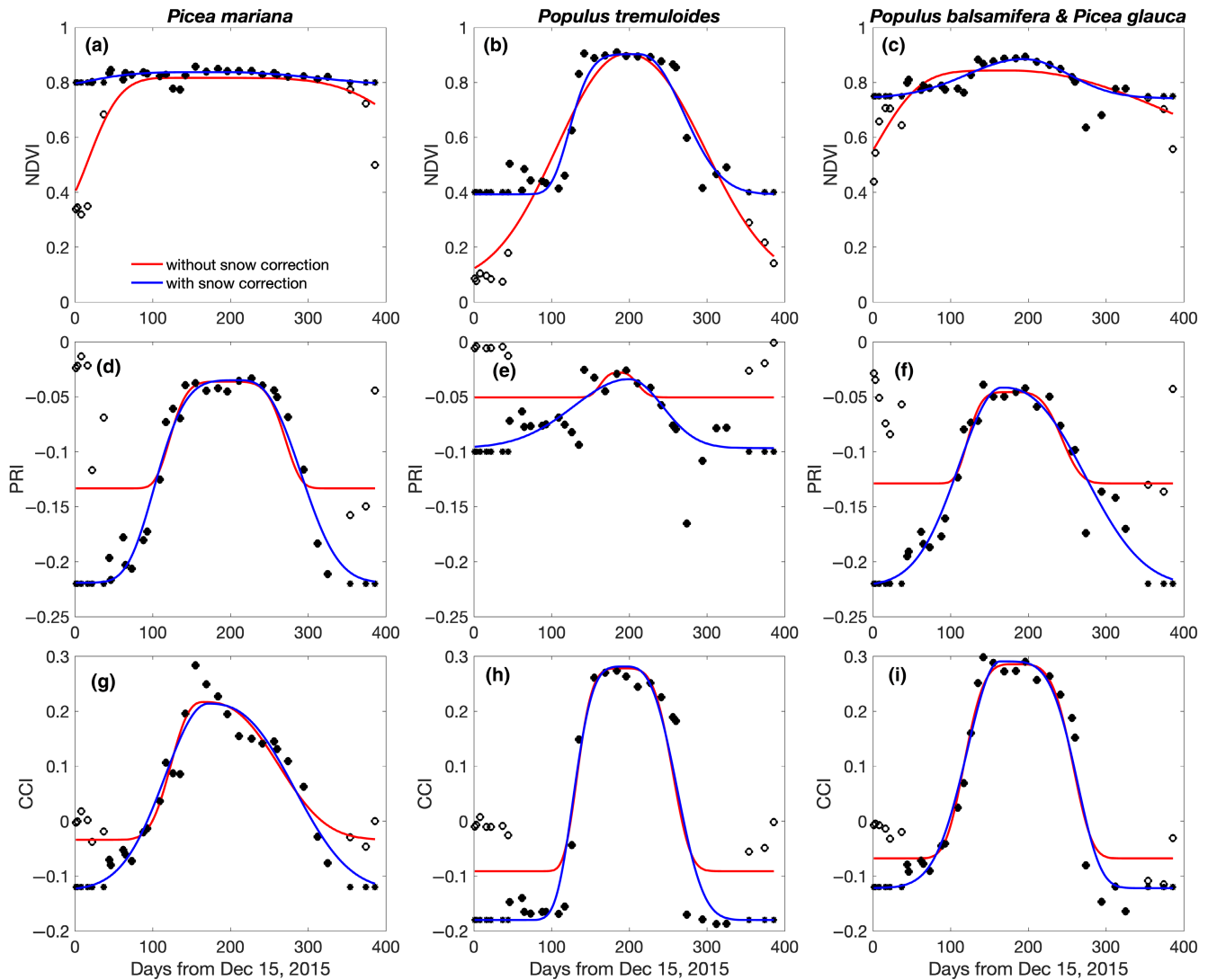
FIGURE 11 Effect of snow and snow removal on phenology of remotely sensed vegetation indices. Examples of one evergreen (*Picea mariana*, a, d, g), one deciduous (*Populus tremuloides*, b, e, h), and one mixed stand (*Populus balsamifera* & *Picea glauca*, c, f, i) are shown. Open points at the beginning and end season indicate snow-affected measurements, identified from digital images. Asterisks indicate snow-corrected values, and solid points indicate snow-free values. Instead of using data from calendar years, we expressed data as "days from December 15, 2015" to include more snow-affected period, due to a relatively short snow season in 2016.

TABLE 2 Snow effects on vegetation index values, season changes, and photosynthetic rate—vegetation index relationships.

VI	VI value	Seasonal change	Photosynthetic rate–VI relationship
NDVI	Decreased	Exaggerated	Exaggerated
PRI	Increased	Reduced	Reduced
CCI	Increased	Reduced	Reduced

Abbreviations: CCI, chlorophyll/carotenoid index; NDVI, normalized difference vegetation index; PRI, photochemical reflectance index; VI, vegetation index.

when leaves were available, which tended to minimize the confounding effects of snow on GPP estimation due to the lack of sampling in the winter and early spring for deciduous trees. In this

experiment, the tree canopies tended to have less snow cover than comparable stands in natural landscapes, in part due to the sun-exposed and slightly warmer rooftop conditions, reducing the snow influence relative to natural landscapes. The relatively tight spacing of plants in synthetic plots likely influenced the retention of snow and likely altered the confounding effect of snow relative to that of natural forests. Larger vegetation has different canopy structure compared to younger trees, which could further influence the retention of snow and alter the exact snow cover impacts in natural landscapes. For these reasons, vegetation indices in this small-scale experiment were likely less sensitive to snow cover than would be apparent in most natural landscapes indicating that this canopy-level experiment probably presented a conservative estimate of the confounding effects of snow. Natural landscapes tend to have more persistent snow cover than observed in this

rooftop experiment, indicating that snow is likely to have even greater confounding effects in satellite observations, as has recently been observed in a parallel study of MODIS satellite data (Wang et al., 2023).

4.4 | Caveats and future work

In addition to the possible differences between our experimental conditions and natural landscapes, several other issues are worth noting when considering the application of snow corrections. Despite the linear relationships between snow cover and vegetation indices reported here (Figure 8), additional attention would likely be required when exploring these precise snow cover effects in natural settings. Since snow cover estimates from imagery will likely vary with view angle, angular effects should also be considered in studies designed to assess snow impacts on remotely sensed signals. For example, images from the PhenoCam Network, are typically taken from oblique angles, which yields a different snow cover estimate than nadir views due to enhanced visibility of vegetation at oblique angles (Brown et al., 2016; Toomey et al., 2015). Snow estimation using images taken at oblique angles typically requires a transformation to orthophotos. The accuracy of snow cover estimation is subject to errors in the transformation and illumination conditions (Fedorov et al., 2016; Hinkler et al., 2002). Combining imagery collected by drone (Belmonte et al., 2021) or CubeSat (Cannistra et al., 2021; John et al., 2022) with machine learning methods may offer new approaches to deriving high spatial resolution snow coverage products. The accuracy of these methods is sensitive to forest canopy structure and landscape topography (Belmonte et al., 2021; Cannistra et al., 2021). In any case, the advent of global network of digital cameras and CubeSat observations hold promising potential for snow estimation, which could further advance the forest productivity estimation using remote sensing by eliminating snow's confounding effects.

5 | CONCLUSIONS

Vegetation indices are widely used in monitoring terrestrial plant photosynthesis and GPP across spatial and temporal scales. We found that vegetation indices from reflectance were all affected by snow cover change, but in different directions and to different degrees. These effects of snow cover on vegetation indices also varied with functional types (evergreen and deciduous) and species (e.g., *Picea* sp. vs. *Pinus* sp.). Snow cover decreased NDVI-based vegetation indices and snow melt in the spring, exaggerating the correlation between NDVI-based vegetation indices and GPP, while the opposite effects were seen for CCI and PRI. These results indicate that large errors can result in GPP estimation for large regions of the world exposed to seasonally varying snow cover, including the boreal and high-altitude regions.

For accurate GPP estimation, these large snow cover effects on vegetation indices and implications for relationships between vegetation indices and productivity should be addressed in any large-scale satellite studies of GPP using these vegetation indices. In particular, the large and contrasting effects of snow on different vegetation indices and for different vegetation types suggest that many models of GPP driven from these indices could have considerable errors, particularly during the critical period of spring snow melt and photosynthetic activation, as has previously been noted (e.g., Richardson et al., 2012; Rogers et al., 2022). Failure to remove the snow effects could lead to incorrect estimations of GPP using either empirical methods between GPP and vegetation indices (Wang et al., 2023) or using machine learning methods (Cheng et al., 2022; Pierrat, Bortnik, et al., 2022; Pierrat, Magney, et al., 2022). Rather than simple linear effects, the influence of snow on vegetation indices are complicated by species, vegetation type, and view angle effects, making simple and accurate snow corrections challenging. These findings of snow and vegetation type effects on vegetation indices have large implications for GPP estimation in boreal forests, where snow cover, species composition, and photosynthetic activity are all changing. While we demonstrate that empirical corrections using snow coverage estimation based on digital imagery can reduce snow artifacts to better reveal the underlying biological effects, the confounding snow effects on reflectance-based vegetation indices and relationships between GPP and these vegetation indices deserve further study if we are to develop and apply reliable methods of accounting for snow cover. This is a particular need for satellite studies of boreal forests, considering the critical role the boreal forests play in regulating the global carbon cycle and its sensitivity to global climate change. Proper correction for snow effects could lead to improved accuracy of GPP assessments for large regions of the world prone to changing snow cover.

AUTHOR CONTRIBUTIONS
Kyle R. Springer, Ran Wang, and John A. Gamon designed the experiments and wrote the manuscript. Kyle R. Springer and Ran Wang performed the experiments and analyzed the data.

CONFLICT OF INTEREST STATEMENT
The authors declare no conflict of interest.

DATA AVAILABILITY STATEMENT
The data that support the findings of this study are openly available in EcoSIS Spectral Library (ecosis.org) at https://doi.org/10.21232/HbGMYtyz and https://doi.org/10.21232/

aY2V7zCr. *Leaf reflectance*: https://ecosis.org/package/leaf-spectra-of-boreal-tree-species-from-alberta-potted-tree-experiment. *Canopy reflectance*: https://ecosis.org/package/b89c301e-aa03-43c3-870e-e29c60ef5716. Reflectance data were processed using MultiSpec, which is available through SpecNet (https://specnet.info/toolkit/).

ORCID

Ran Wang https://orcid.org/0000-0002-3810-9103

John A. Gamon https://orcid.org/0000-0002-8269-7723

REFERENCES

Adams, W. W., III, Demmig-Adams, B., Rosenstiel, T. N., Brightwell, A. K., & Ebbert, V. (2002). The employment of zeaxanthin-dependent photoprotective. *Plant Biology*, 4, 545–557.

Badgley, G., Anderegg, L. D. L., Berry, J. A., & Field, C. B. (2019). Terrestrial gross primary production: Using NIRv to scale from site to globe. *Global Change Biology*, 25, 3731–3740. https://doi.org/10.1111/gcb.14729

Badgley, G., Field, C. B., & Berry, J. A. (2017). Canopy near-infrared reflectance and terrestrial photosynthesis. *Science Advances*, 3(3), e1602244. https://doi.org/10.1126/sciadv.1602244

Balzarolo, M., Vicca, S., Nguy-Robertson, A. L., Bonal, D., Elbers, J. A., Fu, Y. H., Grünwald, T., Horemans, J. A., Papale, D., Peñuelas, J., Suyker, A., & Veroustraete, F. (2016). Matching the phenology of Net Ecosystem Exchange and vegetation indices estimated with MODIS and FLUXNET in-situ observations. *Remote Sensing of Environment*, 174, 290–300. https://doi.org/10.1016/j.rse.2015.12.017

Belmonte, A., Sankey, T., Biederman, J., Bradford, J., Goetz, S., & Kolb, T. (2021). UAV-based estimate of snow cover dynamics: Optimizing semi-arid forest structure for snow persistence. *Remote Sensing*, 13(5). https://doi.org/10.3390/rs13051036

Bokhorst, S., Pedersen, S. H., Brucker, L., Anisimov, O., Bjerke, J. W., Brown, R. D., Ehrich, D., Essery, R. L. H., Heilig, A., Ingvander, S., Johansson, C., Johansson, M., Jónsdóttir, I. S., Inga, N., Luojus, K., Macelloni, G., Mariash, H., McLennan, D., Rosqvist, G. N., … Callaghan, T. V. (2016). Changing Arctic snow cover: A review of recent developments and assessment of future needs for observations, modelling, and impacts. *Ambio*, 45(5), 516–537. https://doi.org/10.1007/s13280-016-0770-0

Bonan, G. B. (2008). Forest and climate change: Forcings, feedbacks, and the climate benefits of forests. *Science*, 320, 1444–1449.

Brandt, J. P., Flannigan, M. D., Maynard, D. G., & Thompson, I. D. (2013). An introduction to Canada's boreal zone: Ecosystem processes, health, sustainability, and environmental issues. *Environmental Reviews*, 226(December), 207–226. https://doi.org/10.1139/Er-2013-0040

Brown, T. B., Hultine, K. R., Steltzer, H., Denny, E. G., Denslow, M. W., Granados, J., Henderson, S., Moore, D., Nagai, S., SanClements, M., Sánchez-Azofeifa, A., Sonnentag, O., Tazik, D., & Richardson, A. D. (2016). Using phenocams to monitor our changing earth: Toward a global phenocam network. *Frontiers in Ecology and the Environment*, 14(2), 84–93. https://doi.org/10.1002/fee.1222

Bunn, A. G., Goetz, S. J., Kimball, J. S., & Zhang, K. (2007). Northern high-latitude ecosystems respond to climate change. *Eos*, 88(34), 333–335. https://doi.org/10.1029/2007EO340001

Camps-Valls, G., Campos-Taberner, M., Moreno-Martínez, Á., Walther, S., Duveiller, G., Cescatti, A., Mahecha, M. D., Muñoz-Marí, J., García-Haro, F. J., Guanter, L., Jung, M., Gamon, J. A., Reichstein, M., & Running, S. W. (2021). A unified vegetation index for quantifying the terrestrial biosphere. *Science Advances*, 7(9), 1–11. https://doi.org/10.1126/sciadv.abc7447

Cannistra, A. F., Shean, D. E., & Cristea, N. C. (2021). High-resolution CubeSat imagery and machine learning for detailed snow-covered area. *Remote Sensing of Environment*, 258(July 2020), 112399. https://doi.org/10.1016/j.rse.2021.112399

Cheng, R., Magney, T. S., Orcutt, E. L., Pierrat, Z., Köhler, P., Bowling, D. R., Bret-Harte, M. S., Euskirchen, E. S., Jung, M., Kobayashi, H., Rocha, A. V., Sonnentag, O., Stutz, J., Walther, S., Zona, D., & Frankenberg, C. (2022). Evaluating photosynthetic activity across Arctic-Boreal land cover types using solar-induced fluorescence. *Environmental Research Letters*, 17(11), 115009. https://doi.org/10.1088/1748-9326/ac9dae

DeFries, R. S., & Townshend, J. R. G. (1994). NDVI-derived land cover classifications at a global scale. *International Journal of Remote Sensing*, 15(17), 3567–3586.

Demmig-Adams, B., & Adams, W. W. (1996). The role of xanthophyll cycle carotenoids in the protection of photosynthesis. *Trends in Plant Science*, 1, 21–26. https://doi.org/10.1016/S1360-1385(96)80019-7

Dial, R. J., Maher, C. T., Hewitt, R. E., & Sullivan, P. F. (2022). Sufficient conditions for rapid range expansion of a boreal conifer. *Nature*, 608(7923), 546–551. https://doi.org/10.1038/s41586-022-05093-2

Dunn, A. L., Barford, C. C., Wofsy, S. C., Goulden, M. L., & Daube, B. C. (2007). A long-term record of carbon exchange in a boreal black spruce forest: Means, responses to interannual variability, and decadal trends. *Global Change Biology*, 13(3), 577–590. https://doi.org/10.1111/j.1365-2486.2006.01221.x

Eklundh, L., Jin, H., Schubert, P., Guzinski, R., & Heliasz, M. (2011). An optical sensor network for vegetation phenology monitoring and satellite data calibration. *Sensors*, 11, 7678–7709. https://doi.org/10.3390/s110807678

Estiarte, M., & Peñuelas, J. (2015). Alteration of the phenology of leaf senescence and fall in winter deciduous species by climate change: Effects on nutrient proficiency. *Global Change Biology*, 21(3), 1005–1017. https://doi.org/10.1111/gcb.12804

Fedorov, R., Member, S., Camerada, A., Fraternali, P., & Tagliasacchi, M. (2016). Estimating snow cover from publicly available images. *IEEE Transactions on Multimedia*, 18(6), 1187–1200.

Gamon, J. A. (2015). Optical sampling of the flux tower footprint. *Biogeosciences Discussions*, 12(6), 4973–5014. https://doi.org/10.5194/bgd-12-4973-2015

Gamon, J. A., & Berry, J. A. (2012). Facultative and constitutive pigment effects on the photochemical reflectance index (PRI) in sun and shade conifer needles. *Israel Journal of Plant Sciences*, 60, 85–95. https://doi.org/10.1560/IJPS.60.1-2.85

Gamon, J. A., Cheng, Y., Claudio, H., MacKinney, L., & Sims, D. A. (2006). A mobile tram system for systematic sampling of ecosystem optical properties. *Remote Sensing of Environment*, 103, 246–254. https://doi.org/10.1016/j.rse.2006.04.006

Gamon, J. A., Field, C. B., Goulden, M. L., Griffin, K. L., Hartley, A. E., Joel, G., Peñuelas, J., & Valentini, R. (1995). Relationships between NDVI, canopy structure, and photosynthesis in three Californian vegetation types. *Ecological Applications*, 5(1), 28–41. https://doi.org/10.2307/1942049

Gamon, J. A., Huemmrich, K. F., Stone, R. S., & Tweedie, C. E. (2013). Spatial and temporal variation in primary productivity (NDVI) of coastal Alaskan tundra: Decreased vegetation growth following earlier snowmelt. *Remote Sensing of Environment*, 129, 144–153. https://doi.org/10.1016/j.rse.2012.10.030

Gamon, J. A., Huemmrich, K. F., Wong, C. Y. S., Ensminger, I., Garrity, S., Hollinger, D. Y., Noormets, A., & Peñuelas, J. (2016). A remotely sensed pigment index reveals photosynthetic phenology in evergreen conifers. *Proceedings of the National Academy of Sciences of the United States of America*, 113(46), 13087–13092. https://doi.org/10.1073/pnas.1606162113

Gamon, J. A., Kovalchuck, O., Wong, C. Y. S., Harris, A., & Garrity, S. R. (2015). Monitoring seasonal and diurnal changes in

photosynthetic pigments with automated PRI and NDVI sensors. *Biogeosciences*, *12*(13), 4149–4159. https://doi.org/10.5194/bg-12-4149-2015

Gamon, J. A., Peñuelas, J., & Field, C. B. (1992). A narrow-waveband spectral index that tracks diurnal changes in photosynthetic efficiency. *Remote Sensing of Environment*, *41*, 35–44. https://doi.org/10.1016/0034-4257(92)90059-S

Gamon, J. A., Serrano, L., & Surfus, S. (1997). The photochemical reflectance index: An optical indicator of photosynthetic radiation use efficiency across species, functional types, and nutrient levels. *Oecologia*, *112*, 492–501.

Garbulsky, M. F., Peñuelas, J., Gamon, J. A., Inoue, Y., & Filella, I. (2011). The photochemical reflectance index (PRI) and the remote sensing of leaf, canopy and ecosystem radiation use efficiencies: A review and meta-analysis. *Remote Sensing of Environment*, *115*(2), 281–297. https://doi.org/10.1016/j.rse.2010.08.023

Gladkova, I., Grossberg, M., Bonev, G., Romanov, P., & Shahriar, F. (2012). Increasing the accuracy of MODIS/aqua snow product using quantitative image restoration technique. *IEEE Geoscience and Remote Sensing Letters*, *9*(4), 740–743. https://doi.org/10.1109/LGRS.2011.2180505

Goetz, S. J., Bunn, A. G., Fiske, G. J., & Houghton, R. A. (2005). Satellite-observed photosynthetic trends across boreal North America associated with climate and fire disturbance. *Proceedings of the National Academy of Sciences of the United States of America*, *102*(38), 13521–13525. https://doi.org/10.1073/pnas.0506179102

Hinkler, J., Pedersen, S. B., Rasch, M., & Hansen, B. U. (2002). Automatic snow cover monitoring at high temporal and spatial resolution, using images taken by a standard digital camera. *International Journal of Remote Sensing*, *23*(21), 4669–4682. https://doi.org/10.1080/01431160110113881

Hmimina, G., Dufrêne, E., Pontailler, J. Y., Delpierre, N., Aubinet, M., Caquet, B., de Grandcourt, A., Burban, B., Flechard, C., Granier, A., Gross, P., Heinesch, B., Longdoz, B., Moureaux, C., Ourcival, J.-M., Rambal, S., André, L. S., & Soudani, K. (2013). Evaluation of the potential of MODIS satellite data to predict vegetation phenology in different biomes: An investigation using ground-based NDVI measurements. *Remote Sensing of Environment*, *132*, 145–158. https://doi.org/10.1016/j.rse.2013.01.010

Hmimina, G., Dufrêne, E., & Soudani, K. (2014). Relationship between photochemical reflectance index and leaf ecophysiological and biochemical parameters under two different water statuses: Towards a rapid and efficient correction method using real-time measurements. *Plant, Cell & Environment*, *37*, 473–487. https://doi.org/10.1111/pce.12171

Huete, A., Didan, K., Miura, T., Rodriguez, E. P., Gao, X., & Ferreira, L. G. (2002). Overview of the radiometric and biophysical performance of the MODIS vegetation indices. *Remote Sensing of Environment*, *83*, 195–213. https://doi.org/10.1016/S0034-4257(02)00096-2

Ikawa, H., Nakai, T., Busey, R. C., Kim, Y., Kobayashi, H., Nagai, S., Ueyama, M., Saito, K., Nagano, H., Suzuki, R., & Hinzman, L. (2015). Understory CO_2, sensible heat, and latent heat fluxes in a black spruce forest in interior Alaska. *Agricultural and Forest Meteorology*, *214-215*, 80–90. https://doi.org/10.1016/j.agrformet.2015.08.247

Intergovernmental Panel on Climate Change. (2007). *Fourth assessment report*. Intergovernmental Panel on Climate Change; Cambridge University Press. www.ipcc.ch, https://doi.org/10.1038/446727a

Jahns, P., & Holzwarth, A. R. (2012). The role of the xanthophyll cycle and of lutein in photoprotection of photosystem II. *Biochimica et Biophysica Acta, Bioenergetics*, *1817*, 182–193. https://doi.org/10.1016/j.bbabio.2011.04.012

Jin, H., & Eklundh, L. (2014). A physically based vegetation index for improved monitoring of plant phenology. *Remote Sensing of Environment*, *152*, 512–525. https://doi.org/10.1016/j.rse.2014.07.010

Jin, H., Jönsson, A. M., Bolmgren, K., Langvall, O., & Eklundh, L. (2017). Disentangling remotely-sensed plant phenology and snow seasonality at northern Europe using MODIS and the plant phenology index. *Remote Sensing of Environment*, *198*, 203–212. https://doi.org/10.1016/j.rse.2017.06.015

John, A., Cannistra, A. F., Yang, K., Tan, A., Shean, D., Hille Ris Lambers, J., & Cristea, N. (2022). High-resolution snow-covered area mapping in forested mountain ecosystems using PlanetScope imagery. *Remote Sensing*, *14*(14), 1–24. https://doi.org/10.3390/rs14143409

Jönsson, P., & Eklundh, L. (2004). TIMESAT—A program for analyzing time-series of satellite sensor data. *Computers and Geosciences*, *30*(8), 833–845. https://doi.org/10.1016/j.cageo.2004.05.006

Keenan, T. F., Baker, I., Barr, A., Ciais, P., Davis, K., Dietze, M., Dragoni, D., Gough, C. M., Grant, R., Hollinger, D., Hufkens, K., Poulter, B., McCaughey, H., Raczka, B., Ryu, Y., Schaefer, K., Tian, H., Verbeeck, H., Zhao, M., & Richardson, A. D. (2012). Terrestrial biosphere model performance for inter-annual variability of land-atmosphere CO_2 exchange. *Global Change Biology*, *18*(6), 1971–1987. https://doi.org/10.1111/j.1365-2486.2012.02678.x

Liu, J., & Pattey, E. (2010). Retrieval of leaf area index from top-of-canopy digital photography over agricultural crops. *Agricultural and Forest Meteorology*, *150*, 1485–1490. https://doi.org/10.1016/j.agrformet.2010.08.002

Lv, Z., & Pomeroy, J. W. (2019). Detecting intercepted snow on mountain needleleaf forest canopies using satellite remote sensing. *Remote Sensing of Environment*, *231*(March), 111222. https://doi.org/10.1016/j.rse.2019.111222

Marsh, P., Bartlett, P., MacKay, M., Pohl, S., & Lantz, T. (2010). Snowmelt energetics at a shrub tundra site in the western Canadian Arctic. *Hydrological Processes*, *24*(25), 3603–3620.

MATLAB. (2022). *Version R2022b*. The MathWorks Inc.

Ménard, C. B., Essery, R., Pomeroy, J., Marsh, P., & Clark, D. B. (2014). A shrub bending model to calculate the albedo of shrub-tundra. *Hydrological Processes*, *28*(2), 341–351.

Moreau, G., Chagnon, C., Auty, D., Caspersen, J., & Achim, A. (2020). Impacts of climatic variation on the growth of black spruce across the forest-tundra ecotone: Positive effects of warm growing seasons and heat waves are offset by late spring frosts. *Frontiers in Forests and Global Change*, *3*(December), 1–14. https://doi.org/10.3389/ffgc.2020.613523

Myers-Smith, I. H., & Hik, D. S. (2013). Shrub canopies influence soil temperatures but not nutrient dynamics: An experimental test of tundra snow-shrub interactions. *Ecology and Evolution*, *3*(11), 3683–3700. https://doi.org/10.1002/ece3.710

Myers-Smith, I. H., Kerby, J. T., Phoenix, G. K., Bjerke, J. W., Epstein, H. E., Assmann, J. J., John, C., Andreu-Hayles, L., Angers-Blondin, S., Beck, P. S. A., Berner, L. T., Bhatt, U. S., Bjorkman, A. D., Blok, D., Bryn, A., Christiansen, C. T., Cornelissen, J. H. C., Cunliffe, A. M., Elmendorf, S. C., … Wipf, S. (2020). Complexity revealed in the greening of the Arctic. *Nature Climate Change*, *10*(2), 106–117. https://doi.org/10.1038/s41558-019-0688-1

Myneni, R. B., Keeling, C. D., Tucker, C. J., Asrar, G., & Nemani, R. R. (1997). Increased plant growth in the northern high latitudes from 1981 to 1991. *Nature*, *386*(April), 698–702.

Negi, H. S., Singh, S. K., & Kulkarni, A. V. (2009). Spectral reflectance measurements in snowbound areas of Indian Himalayas. In S. Rajendra, S. Aravindan, T. Jeyavel Rajakumar, R. Sivakumar, & K. R. Murali Mohan (Eds.), *Hyperspectral remote sensing and spectral signature applications* (pp. 109–120). NIPA.

Niyogi, K. K., Björkman, O., & Grossman, A. R. (1997). The roles of specific xanthophylls in photoprotection. *Proceedings of the National Academy of Sciences of the United States of America*, *94*, 14162–14167. https://doi.org/10.1073/pnas.94.25.14162

Öquist, G., & Huner, N. P. A. (2003). Photosynthesis of overwintering evergreen plants. *Annual Review of Plant Biology*, *54*, 329–355. https://doi.org/10.1146/annurev.arplant.54.072402.115741

Pierrat, Z., Magney, T., Parazoo, N. C., Grossmann, K., Bowling, D. R., Seibt, U., Johnson, B., Helgason, W., Barr, A., Bortnik, J., Norton,

A., Maguire, A., Frankenberg, C., & Stutz, J. (2022). Diurnal and seasonal dynamics of solar-induced chlorophyll fluorescence, vegetation indices, and gross primary productivity in the boreal forest. *Journal of Geophysical Research: Biogeosciences*, 127(2), e2021JG006588. https://doi.org/10.1029/2021JG006588

Pierrat, Z., Nehemy, M. F., Roy, A., Magney, T., Parazoo, N. C., Laroque, C., Pappas, C., Sonnentag, O., Grossmann, K., Bowling, D. R., Seibt, U., Ramirez, A., Johnson, B., Helgason, W., Barr, A., & Stutz, J. (2021). Tower-based remote sensing reveals mechanisms behind a two-phased spring transition in a mixed-species boreal forest. *Journal of Geophysical Research – Biogeosciences*, 126, 1–20. https://doi.org/10.1029/2020JG006191

Pierrat, Z. A., Bortnik, J., Johnson, B., Barr, A., Magney, T., Bowling, D. R., Parazoo, N., Frankenberg, C., Seibt, U., & Stutz, J. (2022). Forests for forests: Combining vegetation indices with solar-induced chlorophyll fluorescence in random forest models improves gross primary productivity prediction in the boreal forest. *Environmental Research Letters*, 17, 125006. https://doi.org/10.1088/1748-9326/aca5a0

Pomeroy, J. W., Bewley, D. S., Essery, R. L. H., Hedstrom, N. R., Link, T., Granger, R. J., Sicart, J. E., Ellis, C. R., & Janowicz, J. R. (2006). Shrub tundra snowmelt. *Hydrological Processes*, 20(4), 923–941. https://doi.org/10.1002/hyp.6124

Pomeroy, J. W., Gray, D. M., Hedstrom, N. R., & Janowicz, J. R. (2002). Prediction of seasonal snow accumulation in cold climate forests. *Hydrological Processes*, 16(18), 3543–3558. https://doi.org/10.1002/hyp.1228

Ray, P. M., & Bret-Harte, M. S. (2022). Cryocampsis: A biophysical freeze-bending response of shrubs and trees under snow loads. *PNAS Nexus*, 1(4), pgac131.

Richardson, A. D., Anderson, R. S., Arain, M. A., Barr, A. G., Bohrer, G., Chen, G., Chen, J. M., Ciais, P., Davis, K. J., Desai, A. R., Dietze, M. C., Dragoni, D., Garrity, S. R., Gough, C. M., Grant, R., Hollinger, D. Y., Margolis, H. A., McCaughey, H., Migliavacca, M., … Xue, Y. (2012). Terrestrial biosphere models need better representation of vegetation phenology: Results from the North American carbon program site synthesis. *Global Change Biology*, 18(2), 566–584.

Riggs, G. A., Hall, D., & Román, M. O. (2016). *MODIS snow products collection 6 user guide*. https://modis-snow-ice.gsfc.nasa.gov/uploads/C6_MODIS_Snow_User_Guide.pdf

Rogers, A., Serbin, S. P., & Way, D. A. (2022). Reducing model uncertainty of climate change impacts on high latitude carbon assimilation. *Global Change Biology*, 28(4), 1222–1247. https://doi.org/10.1111/gcb.15958

Running, S. W., Nemani, R. R., Heinsch, F. A., Zhao, M., Reeves, M., & Hashimoto, H. (2004). A continuous satellite-derived measure of global terrestrial primary production. *BioScience*, 54(6), 547–560. https://doi.org/10.1641/0006-3568(2004)054[0547:ACSMOG]2.0.CO;2

Ryu, Y., Berry, J. A., & Baldocchi, D. D. (2019). What is global photosynthesis? History, uncertainties and opportunities. *Remote Sensing of Environment*, 223(January), 95–114. https://doi.org/10.1016/j.rse.2019.01.016

Saha, A., Garg, P. K., & Patil, M. (2019). The effect of contaminated snow reflectance using hyperspectral remote sensing—A review. *International Journal of Image and Data Fusion*, 10, 107–130. https://doi.org/10.1080/19479832.2019.1582561

Schaefer, K., Schwalm, C. R., Williams, C., Arain, M. A., Barr, A., Chen, J. M., Davis, K. J., Dimitrov, D., Hilton, T. W., Hollinger, D. Y., Humphreys, E., Poulter, B., Raczka, B. M., Richardson, A. D., Sahoo, A., Thornton, P., Vargas, R., Verbeeck, H., Anderson, R., … Zhou, X. (2012). A model-data comparison of gross primary productivity: Results from the North American Carbon Program site synthesis. *Journal of Geophysical Research – Biogeosciences*, 117(G3). https://doi.org/10.1029/2012JG001960

Schimel, D., Pavlick, R., Fisher, J. B., Asner, G. P., Saatchi, S., Townsend, P., Miller, C., Frankenberg, C., Hibbard, K., & Cox, P. (2015). Observing terrestrial ecosystems and the carbon cycle from space. *Global Change Biology*, 21(5), 1762–1776. https://doi.org/10.1111/gcb.12822

Schimel, D., & Schneider, F. D. (2019). Flux towers in the sky: Global ecology from space. *New Phytologist*, 224(2), 570–584. https://doi.org/10.1111/nph.15934

Singh, S. K., Kulkarni, A. V., & Chaudhary, B. S. (2010). Hyperspectral analysis of snow reflectance to understand the effects of contamination and grain size. *Annals of Glaciology*, 51, 83–88. https://doi.org/10.3189/172756410791386535

Springer, K. R. (2018). *Monitoring phenology of boreal trees using remote sensing* (Master of Science thesis). University of Alberta. Education and Research Archive at the University of Alberta. https://doi.org/10.7939/R3K64B87T

Springer, K. R., Wang, R., & Gamon, J. A. (2017). Parallel seasonal patterns of photosynthesis, fluorescence, and reflectance indices in boreal trees. *Remote Sensing*, 9(7), 1–18. https://doi.org/10.3390/rs9070691

Toomey, M., Friedl, M. A., Frolking, S., Hufkens, K., Klosterman, S., Sonnentag, O., Baldocchi, D. D., Bernacchi, C. J., Biraud, S. C., Bohrer, G., Brzostek, E., Burns, S. P., Coursolle, C., Hollinger, D. Y., Margolis, H. A., Mccaughey, H., Monson, R. K., Munger, J. W., Pallardy, S., … Richardson, A. D. (2015). Greenness indices from digital cameras predict the timing and seasonal dynamics of canopy-scale photosynthesis. *Ecological Applications*, 25(1), 99–115. https://doi.org/10.1890/14-0005.1

Tucker, C. J. (1979). Red and photographic infrared linear combinations for monitoring vegetation. *Remote Sensing of Environment*, 8, 127–150. https://doi.org/10.1016/0034-4257(79)90013-0

Walker, X., & Johnstone, J. F. (2014). Widespread negative correlations between black spruce growth and temperature across topographic moisture gradients in the boreal forest. *Environmental Research Letters*, 9(6). https://doi.org/10.1088/1748-9326/9/6/064016

Wang, R., Bowlling, D. R., Gamon, J. A., Smith, K. R., Yu, R., Hmimina, G., Ueyama, M., Noormets, A., Kolb, T. E., Richardson, A. D., Bourque, C. P.-A., Braho, R., Blanken, P. D., Black, T. A., & Altaf Arain, M. (2023). Snow-corrected vegetation indices for improved gross primary productivity assessment in North American evergreen forests. *Agricultural and Forest Meteorology*, 340, 109600. https://doi.org/10.1016/j.agrformet.2023.109600

Wang, R., Springer, K. R., & Gamon, J. A. (2016a). *Leaf spectra of boreal tree species from Alberta potted tree experiment*. Data set. Ecological Spectral Information System (EcoSIS). http://ecosis.org. https://doi.org/10.21232/HbGMYtyz

Wang, R., Springer, K. R., & Gamon, J. A. (2016b). *Canopy spectra of boreal tree species from Alberta potted tree experiment*. Data set. Ecological Spectral Information System (EcoSIS). http://ecosis.org. https://doi.org/10.21232/aY2V7zCr

Wang, X., Wang, J., Che, T., Huang, X., Hao, X., & Li, H. (2018). Snow cover mapping for complex mountainous forested environments based on a multi-index technique. *IEEE Journal of Selected Topics in Applied Earth Observations and Remote Sensing*, 11(5), 1433–1441. https://doi.org/10.1109/JSTARS.2018.2810094

Way, D. A., & Oren, R. (2010). Differential responses to changes in growth temperature between trees from different functional groups and biomes: A review and synthesis of data. *Tree Physiology*, 30(6), 669–688. https://doi.org/10.1093/treephys/tpq015

Way, D. A., Oren, R., & Kroner, Y. (2015). The space-time continuum: The effects of elevated CO_2 and temperature on trees and the importance of scaling. *Plant, Cell & Environment*, 38(6), 991–1007. https://doi.org/10.1111/pce.12527

White, J. C., Wulder, M. A., Hermosilla, T., Coops, N. C., & Hobart, G. W. (2017). A nationwide annual characterization of 25 years of forest disturbance and recovery for Canada using Landsat time

series. *Remote Sensing of Environment*, *194*, 303–321. https://doi.org/10.1016/j.rse.2017.03.035

Wong, C. Y. S., D'Odorico, P., Arain, M. A., & Ensminger, I. (2020). Tracking the phenology of photosynthesis using carotenoid-sensitive and near-infrared reflectance vegetation indices in a temperate evergreen and mixed deciduous forest. *New Phytologist*, *226*(6), 1682–1695. https://doi.org/10.1111/nph.16479

Wong, C. Y. S., D'Odorico, P., Bhathena, Y., Arain, M. A., & Ensminger, I. (2019). Carotenoid based vegetation indices for accurate monitoring of the phenology of photosynthesis at the leaf-scale in deciduous and evergreen trees. *Remote Sensing of Environment*, *233*(November), 111407. https://doi.org/10.1016/j.rse.2019.111407

Wong, C. Y. S., & Gamon, J. A. (2015a). The photochemical reflectance index provides an optical indicator of spring photosynthetic activation in evergreen conifers. *New Phytologist*, *206*, 196–208. https://doi.org/10.1111/nph.13251

Wong, C. Y. S., & Gamon, J. A. (2015b). Three causes of variation in the photochemical reflectance index (PRI) in evergreen conifers. *New Phytologist*, *206*, 187–195. https://doi.org/10.1111/nph.13159

Wong, C. Y. S., Mercado, L. M., Arain, M. A., & Ensminger, I. (2022). Remotely sensed carotenoid dynamics improve modelling photosynthetic phenology in conifer and deciduous forests. *Agricultural and Forest Meteorology*, *321*(October 2021), 108977. https://doi.org/10.1016/j.agrformet.2022.108977

Wu, C., Gonsamo, A., Gough, C. M., Chen, J. M., & Xu, S. (2014). Modeling growing season phenology in North American forests using seasonal mean vegetation indices from MODIS. *Remote Sensing of Environment*, *147*, 79–88. https://doi.org/10.1016/j.rse.2014.03.001

Xiao, J., Chevallier, F., Gomez, C., Guanter, L., Hicke, J. A., Huete, A. R., Ichii, K., Ni, W., Pang, Y., Rahman, A. F., Sun, G., Yuan, W., Zhang, L., & Zhang, X. (2019). Remote sensing of the terrestrial carbon cycle: A review of advances over 50 years. *Remote Sensing of Environment*, *233*(January), 111383. https://doi.org/10.1016/j.rse.2019.111383

Yang, J. C., Magney, T. S., Albert, L. P., Richardson, A. D., Frankenberg, C., Stutz, J., Grossmann, K., Burns, S. P., Seyednasrollah, B., Blanken, P. D., & Bowling, D. R. (2022). Gross primary production (GPP) and red solar induced fluorescence (SIF) respond differently to light and seasonal environmental conditions in a subalpine conifer forest. *Agricultural and Forest Meteorology*, *317*(June 2021), 108904. https://doi.org/10.1016/j.agrformet.2022.108904

Yang, J. C., Magney, T. S., Yan, D., Knowles, J. F., Smith, W. K., Scott, R. L., & Barron-Gafford, G. A. (2020). The photochemical reflectance index (PRI) captures the ecohydrologic sensitivity of a semiarid mixed conifer forest. *Journal of Geophysical Research – Biogeosciences*, *125*(11), 1–18. https://doi.org/10.1029/2019JG005624

Zeng, Y., Hao, D., Huete, A., Dechant, B., Berry, J., Chen, J. M., Joiner, J., Frankenberg, C., Bond-Lamberty, B., Ryu, Y., Xiao, J., Asrar, G. R., & Chen, M. (2022). Optical vegetation indices for monitoring terrestrial ecosystems globally. *Nature Reviews Earth and Environment*, *3*(7), 477–493. https://doi.org/10.1038/s43017-022-00298-5